

## COMPUTING COMPLETE LYAPUNOV FUNCTIONS FOR DISCRETE-TIME DYNAMICAL SYSTEMS

PETER GIESL AND ZACHARY LANGHORNE

Department of Mathematics, University of Sussex  
Falmer BN1 9QH, United Kingdom

CARLOS ARGÁEZ AND SIGURDUR HAFSTEIN

Faculty of Physical Sciences, University of Iceland  
107 Reykjavík, Iceland

**ABSTRACT.** A complete Lyapunov function characterizes the behaviour of a general discrete-time dynamical system. In particular, it divides the state space into the chain-recurrent set where the complete Lyapunov function is constant along trajectories and the part where the flow is gradient-like and the complete Lyapunov function is strictly decreasing along solutions. Moreover, the level sets of a complete Lyapunov function provide information about attractors, repellers, and basins of attraction.

We propose two novel classes of methods to compute complete Lyapunov functions for a general discrete-time dynamical system given by an iteration. The first class of methods computes a complete Lyapunov function by approximating the solution of an ill-posed equation for its discrete orbital derivative using meshfree collocation. The second class of methods computes a complete Lyapunov function as solution of a minimization problem in a reproducing kernel Hilbert space. We apply both classes of methods to several examples.

**1. Introduction.** We will consider a general autonomous discrete-time dynamical system, described by the iteration of a given function  $g: \mathbb{R}^d \rightarrow \mathbb{R}^d$ :

$$x_{n+1} = g(x_n), \quad (1)$$

where  $x_0 \in \mathbb{R}^d$  is a fixed initial value. We assume that the function  $g$  is continuous, but will require more smoothness later. We call the sequence  $(x_0, x_1, x_2, \dots)$  the trajectory starting at  $x_0$ .

We are interested in the dynamics of (1) for different initial conditions. In dynamical systems, the phase space  $\mathbb{R}^d$  can be distinguished into two different parts with fundamentally different dynamical behaviour: the chain-recurrent set where infinitesimal perturbations can make the flow recurrent and its complement where the flow is gradient-like and robust with respect to perturbations.

The chain-recurrent set  $R$  is the intersection of all local attractor and repeller pairs. A point is in the chain-recurrent set, if every  $\varepsilon$ -trajectory through it comes back to the point after any given time. An  $\varepsilon$ -trajectory is close to a true trajectory

---

2020 *Mathematics Subject Classification.* Primary: 93D30, 65D12, 65K10; Secondary: 39A30.

*Key words and phrases.* Discrete-time dynamical system, complete Lyapunov function, quadratic programming, meshfree collocation.

The research in this paper was supported by the Icelandic Research Fund (Rannís) grant number 163074-052, Complete Lyapunov functions: Efficient numerical computation.

of the system. This indicates (almost) recurrent motion; for a precise definition see, e.g. [13, 23, 24, 25, 26]. The dynamics in the gradient-like regime are transient.

This distinction into the two sets as well as additional behaviour of solutions of (1) can be characterized by a complete Lyapunov function (CLF) [13]. A CLF is a function  $V: \mathbb{R}^d \rightarrow \mathbb{R}$  which is strictly decreasing along trajectories outside the chain-recurrent set  $R$ ,  $V(R)$  is a compact, nowhere dense subset of  $\mathbb{R}$ , and the level sets of  $V$  in  $R$ ,  $V^{-1}(r) \cap R \neq \emptyset$ , are the chain-transitive components of  $R$ .

This implies that a CLF is non-increasing along all trajectories. This property can be expressed by  $\Delta V(x) \leq 0$  where  $\Delta V(x) = V(g(x)) - V(x)$  denotes the discrete orbital “derivative”, i.e. the difference between  $V(x_{n+1})$  and  $V(x_n)$ . The values and level sets of a CLF provide additional information about the dynamics and the long-term behaviour of the system, e.g. an asymptotically stable equilibrium is a local minimum of any CLF.

The first proof of the existence of CLFs for dynamical systems was given by Conley [13] for ODEs on compact metric spaces. Conley’s proof considers each corresponding attractor-repeller pair and constructs a function which is 1 on the repeller, 0 on the attractor and decreasing in between. Then these functions are summed up over all attractor-repeller pairs. Later, Hurley generalized these ideas to more general spaces [24, 26]. These functions, however, are just continuous functions. The existence of smooth CLFs for ODEs on compact spaces was shown in [15] and on noncompact spaces in [32] using results on cone-fields from [9]. Note that results on CLFs for ODEs and discrete-time systems are strongly related since a CLF for an ODE is also a CLF for its time- $T$  map. For further results on CLFs, cf. [16, 24, 26, 31, 1, 30] and [29], where this result is referred to as the *Fundamental Theorem of Dynamical Systems*.

We will call any function that satisfies  $\Delta V(x) \leq 0$  a *complete Lyapunov function candidate*, abbreviated *CLF candidate*. The area of the phase space where  $\Delta V(x) = 0$  holds contains the chain-recurrent set, and the area where  $\Delta V(x) < 0$  holds displays gradient-flow behaviour. The larger the area where  $\Delta V(x) < 0$  holds, the more information on the flow and location of the chain-recurrent set we obtain from a CLF candidate. Note that a constant function is trivially a CLF candidate which, however, does not provide any information about the dynamics. A CLF candidate resembles the Lyapunov functions considered by Auslander [7].

In the following we will propose methods to compute CLF candidates, ideally with a large area, where  $\Delta V(x) < 0$  holds.

Let us first review computational approaches to construct CLF candidates for continuous-time dynamical systems, given by an autonomous ODE of the form  $\dot{x} = f(x)$ . In [28, 8, 22] the state space was subdivided into cells, defining a discrete-time system given by the multivalued time- $T$  map between them, which was computed using the computer package GAIO [14]. An approximate complete Lyapunov function was constructed using graph algorithms for the time- $T$  map in [8]. This approach requires a high number of cells even for low dimensions.

In [10], a CLF was constructed as a continuous piecewise affine (CPA) function, affine on a fixed simplicial complex.

In [2, 4, 5] a CLF was computed by approximately solving the PDE

$$V'(x) = \nabla V(x) \cdot f(x) = -1 \quad (2)$$

using meshfree collocation, in particular using Radial Basis Functions. This is inspired by constructing classical Lyapunov functions for an equilibrium [17, 20].

However, (2) cannot be fulfilled at all points in the chain-recurrent set. Meshfree collocation still constructs an approximation, but error estimates are not available, as they compare the approximation to the solution of the problem, which does not exist. The method is able to detect the chain-recurrent set as the area of the state space where the approximation fails. The method has been improved in several ways, for example, an iteration was proposed to use the information about the chain-recurrent set to then formulate a new PDE for a complete Lyapunov function, which can again be approximated.

Let  $\Omega \subseteq \mathbb{R}^d$  be a bounded domain with Lipschitz boundary. In [18] the problem

$$\begin{cases} \text{minimize} & \|V\|_H, \\ \text{such that} & V'(x) = -1 \text{ for } x \in \Omega_-, \\ & V'(x) \leq 0 \text{ for } x \in \Omega \setminus \Omega_-, \end{cases} \quad (3)$$

was considered, where  $\Omega_-$  is a subset of the state space where the flow is gradient-like. The advantage of this method is that a solution of this problem exists and it suffices to know any subset of the gradient-flow part. The computation of an approximate solution was obtained as the norm-minimal solution in a reproducing kernel Hilbert space after discretization.

Finally, in [19] the following problem was considered

$$\begin{cases} \text{minimize} & \|V\|_H^2 + \int_{\Omega} V'(x) dx, \\ \text{such that} & V'(x) \leq 0 \text{ for all } x \in \Omega \end{cases} \quad (4)$$

It was shown that the problem has a unique solution and any sequence of solutions to discretized problems with finer and finer subdivisions of  $\Omega$  converges strongly to the unique solution. These discretized problems can be formulated as quadratic programming problems and solved efficiently.

In this paper, we will consider these methods for the computation of CLF candidates for continuous-time dynamical systems and adapt them to discrete-time systems. While some aspects are straight-forward, others require new ideas and considerations due to the different nature of discrete-time systems. In particular, the non-locality of the dynamics of discrete-time systems, i.e. the jumps in the system state, requires different techniques to be applied. We will consider and compare the construction of CLF candidates for discrete-time systems by approximating the solution of the equation  $\Delta V(x) = -1$  as well with the methods (3) and (4) using quadratic programming.

Let us give an overview over the contents: In Section 2 we recall the definition of reproducing kernel Hilbert spaces. In Section 3 we propose a method to approximate the solution of  $\Delta V(x) = -1$  in a reproducing kernel Hilbert space using meshfree collocation. In Section 4 we introduce two optimization methods using quadratic programming to compute CLF candidates. One uses equality and inequality constraints, minimizing the norm of the function. The other one minimizes a combination of the norm and the sum of discrete orbital derivatives, and uses only inequality constraints. In Section 5 we apply the methods to several examples and compare the results.

**2. Reproducing kernel Hilbert spaces.** We give a very short introduction to reproducing kernel Hilbert spaces (RKHS) as needed in this paper; for references see [6, 34]. Let  $\Omega \subseteq \mathbb{R}^d$  be a nonempty, bounded domain with Lipschitz boundary and let  $H(\Omega)$  be a Hilbert space of functions  $f : \Omega \rightarrow \mathbb{R}$ .

**Definition 2.1.** A Hilbert space  $H = H(\Omega)$  with inner product  $\langle \cdot, \cdot \rangle_H$  is called a *reproducing kernel Hilbert space (RKHS)* if there is a function  $\Phi : \Omega \times \Omega \rightarrow \mathbb{R}$  with

1.  $\Phi(\cdot, x) \in H$  for all  $x \in \Omega$
2.  $f(x) = \langle f(\cdot), \Phi(\cdot, x) \rangle_H$  for all  $f \in H$  and all  $x \in \Omega$ .

The function  $\Phi$  is called the *reproducing kernel* of  $H$ .

The reproducing kernel is called positive definite, if for any set of pairwise distinct points  $\{x_1, \dots, x_N\} \subseteq \Omega$  the matrix  $(\Phi(x_i, x_j))_{i,j=1,\dots,N}$  is positive definite.

In a RKHS the Riesz representative of a functional  $\lambda \in H^*$  is given by applying it to one argument of the kernel, i.e., by  $\lambda^y \Phi(\cdot, y)$ , where the superscript  $y$  denotes the application of  $\lambda$  with respect to  $y$ . Moreover, we have for  $\lambda, \mu \in H^*$

$$\lambda^x \mu^y \Phi(x, y) = \langle \lambda^x \Phi(\cdot, x), \mu^y \Phi(\cdot, y) \rangle_H. \quad (5)$$

The reproducing kernel of a RKHS is unique. The Sobolev space  $H = H^\sigma(\Omega)$  with  $\sigma > d/2$  is a RKHS, and one can choose a positive definite reproducing kernel of a space that is norm-equivalent to  $H^\sigma(\Omega)$ , see [19, Lemma 2.2]. For example, Wendland's compactly supported radial basis function  $\psi_{l,k} : \mathbb{R}_0^+ \rightarrow \mathbb{R}$  with  $l = \lfloor \frac{d}{2} \rfloor + k + 1$ ,  $k \in \mathbb{N}$ , defines a translation-invariant reproducing kernel by  $\Phi(x, y) = \psi_{l,k}(c\|x - y\|_2)$  with  $c > 0$ ; the corresponding RKHS with this kernel restricted to  $\Omega^2$  consists of the functions in  $H^\sigma(\Omega)$  with  $\sigma = k + \frac{d+1}{2}$ , and the space is norm-equivalent to  $H^\sigma(\Omega)$ , see [33]. If Hilbert spaces  $H_1$  and  $H_2$  consist of the same elements and have scalar products that induce equivalent norms, then we write  $H_1 \cong H_2$ .

**3. Approximate solution of an ill-posed equation.** In this section we seek to adapt the methods of [2, 4, 5, 3] to discrete-time systems. We want to find an approximate solution to the ill-posed equation

$$\Delta V(x) = -1. \quad (6)$$

Note that this equation does not have a solution for all points  $x$  in the chain-recurrent set, and thus we expect the approximation to be poor in these areas. The idea is to use this feature to localize the chain-recurrent set. Note that this only works if our hypothesis is true, that the approximation is notably worse close to the chain-recurrent set than further away.

**3.1. Meshfree collocation.** We will introduce a method to approximate the solution of (6) via meshfree collocation. We fix a bounded domain  $\emptyset \neq \Omega \subseteq \mathbb{R}^d$  and a bounded domain  $S \subseteq \mathbb{R}^d$  with Lipschitz boundary, such that  $\Omega \cup g(\Omega) \subseteq S$ . Since  $\Omega$  and thus  $g(\Omega)$  are bounded,  $S$  can be chosen as  $B_R = \{x \in \mathbb{R}^d \mid \|x\|_2 < R\}$  with sufficiently large  $R > 0$ . We consider a RKHS  $H$  containing  $C^0(S)$ .

Problem (6) is a special version of the following, more general problem with  $r \equiv -1$  and  $L(V) = \Delta V$ :

given a continuous function  $r : \Omega \rightarrow \mathbb{R}$ , and a linear operator  $L : H \rightarrow C^0$ , determine a  $V \in H$  that solves  $LV = r$ .

In order to approximately solve this problem, we discretize it by defining a set of pairwise distinct collocation points  $X = \{x_1, \dots, x_N\} \subseteq \Omega$  and define  $\lambda_i = \delta_{x_i} \circ L$  as well as  $r_i = r(x_i)$ . This defines a finite number of linear operators  $\lambda_1, \dots, \lambda_N \in H^*$  and values  $r_1, \dots, r_N \in \mathbb{R}$ . We assume that the  $\lambda_i$  are linearly independent, and

will derive conditions on the points  $x_i$  to achieve this later. We determine the norm-minimal interpolant of this data in  $H$ , i.e.

$$\min\{\|v\|_H : \lambda_i(v) = r_i \text{ for } i = 1, \dots, N\}. \quad (7)$$

It turns out that the interpolant is given by a linear combination of the Riesz representatives of the  $\lambda_i$ , see [34, Theorem 16.1]. In the case of a RKHS, the Riesz representatives can be expressed in terms of the kernel  $\Phi : S^2 \rightarrow \mathbb{R}$ . Then the solution of (7) is given by

$$v(x) = \sum_{j=1}^N \alpha_j \lambda_j^y \Phi(x, y), \quad (8)$$

where the superscript  $y$  denotes the application of the operator  $\lambda_j$  with respect to  $y$  and the  $\alpha_i \in \mathbb{R}$  are such that  $\lambda_i(v) = r_i$  for all  $i = 1, \dots, N$ , which is equivalent to

$$A\alpha = r, \quad (9)$$

with  $A = (a_{ij})_{i,j=1,\dots,N}$ ,  $r = (r_i)_{i=1,\dots,N}$  and

$$a_{ij} = \lambda_i^x \lambda_j^y \Phi(x, y).$$

If the problem  $LV = r$  has a solution, then error estimates in terms of the fill distance  $h_{X,\Omega} = \sup_{y \in \Omega} \min_{x \in X} \|x - y\|_2$  are available on  $\|LV - Lv\|_H$ , where  $v$  denotes the norm minimal approximation. The fill distance is a measure of how dense the collocation points  $X$  are in  $\Omega$ . Note that since the function evaluation functional is continuous in a RKHS, an estimate  $\|LV - Lv\|_H$  in the norm on  $H$  delivers a point-wise bound on  $|LV(x) - Lv(x)|$ .

In our case, we consider the equation (6), which does not have a solution. While the norm-minimal interpolant of the data can still be determined as described above and (9) has a unique solution, the error estimates cannot be applied, since a solution  $V$  to  $LV = r$  does not exist.

We choose the kernel  $\Phi$  for our reproducing kernel Hilbert space to be a compactly supported kernel given by a Wendland function, i.e.  $\Phi(x, y) = \phi(\|x - y\|_2)$  where  $\phi(r) = \psi_{l,k}(c \cdot r)$  with  $c > 0$  and  $\psi_{l,k}$  is a Wendland function, see Section 2. Then the corresponding RKHS  $H$  of functions  $S \rightarrow \mathbb{R}$ , where  $S$  is bounded and has a Lipschitz boundary and with  $\Phi$  restricted to  $S^2$ , is norm-equivalent to the Sobolev space  $H^\sigma(S)$  with  $\sigma = k + \frac{d+1}{2}$  as discussed above. That is  $H \cong H^\sigma(S)$ .

We fix a finite number of pairwise distinct collocation points  $X = \{x_1, \dots, x_N\} \subseteq \mathbb{R}^d$  and define  $\lambda_i = \delta_{x_i} \circ \Delta$ , i.e.

$$\lambda_i(v) = v(g(x_i)) - v(x_i).$$

We further assume that  $X$  does not contain any fixed point nor any entire periodic orbit of (1). This implies that the  $\lambda_i$  are linearly independent, see the following lemma, and, in particular, that the collocation matrix  $A$  is nonsingular.

**Lemma 3.1.** *Let  $\Omega, S \neq \emptyset$  be bounded domains in  $\mathbb{R}^d$ , such that  $S$  has a Lipschitz boundary and  $\Omega, g(\Omega) \subseteq S$ . Let  $H \cong H^\sigma(S)$  be a RKHS with  $\sigma > d/2$  as above. Let  $X = \{x_1, x_2, \dots, x_N\} \subseteq \Omega$  be a set of  $N$  pairwise distinct points, that does not contain any fixed point or entire periodic orbit of (1), i.e., if  $y_1, y_2, \dots, y_p$  is a  $p$ -periodic orbit,  $p \in \mathbb{N}$  of (1), then there is at least one point of the periodic orbit, that is not in  $X$ .*

Then the set of operators  $\lambda_i = \delta_{x_i} \circ \Delta$ ,  $i = 1, \dots, N$ , is in  $H^*$  and linearly independent. Further, the collocation matrix  $A$  with  $a_{ij} = \lambda_i^x \lambda_j^y \Phi(x, y)$  is positive definite and in particular nonsingular.

*Proof.* First of all, note that  $\lambda_i \in H^*$ . Indeed, note that  $x_i, g(x_i) \in S$  and thus

$$\begin{aligned} |\lambda_i(h)| &\leq |h(g(x_i)) - h(x_i)| \\ &\leq |\langle h(\cdot), \Phi(\cdot, g(x_i)) \rangle_H| + |\langle h(\cdot), \Phi(\cdot, x_i) \rangle_H| \\ &\leq \|h\|_H (\|\Phi(\cdot, g(x_i))\|_H + \|\Phi(\cdot, x_i)\|_H) \\ &= \|h\|_H (\sqrt{\Phi(g(x_i), g(x_i))} + \sqrt{\Phi(x_i, x_i)}) \text{ see (5)} \\ &= 2\sqrt{\phi(0)} \|h\|_H \\ &= C \|h\|_H, \end{aligned}$$

where we have used a RKHS  $H$  with a translation-invariant reproducing kernel  $\Phi(x, y) = \phi(\|x - y\|_2)$ . The statement is correct for any other  $H \cong H^\sigma(S)$  with a different constant.

Now we assume that  $\sum_{i=1}^N d_i \lambda_i = 0$  and show that all  $d_i = 0$ . Let  $x \in X$  be such that  $x \notin g(X)$ .

Let us first show that such a point exists. If for all points  $x \in X$  there was a point  $y \in X$  with  $x = g(y)$ , then we can construct a sequence of points  $y_0 = x$ ,  $y_{-1} = y$ , etc. such that  $g(y_k) = y_{k+1}$ . Since there are finitely many points in  $X$ , there is a (minimal)  $K \in \mathbb{N}$  such that  $y_{-K}$  is one of the previous points of the sequence, i.e.  $y_{-K} = y_{-L}$  with  $\mathbb{N} \ni L \leq K$ . This means that  $X$  contains a fixed point or an entire periodic orbit, namely  $y_{-K}, y_{-K+1}, \dots, y_{-L} = y_{-K}$ , in contradiction to the assumption.

Since  $x = x_k \in X$ ,  $x \notin g(X)$  and all points in  $X$  are pairwise distinct, there is a  $\delta > 0$  such that  $B_\delta(x)$  does not contain any points in  $g(X)$  or  $X \setminus \{x\}$ . Let  $h \in C_0^\infty(\mathbb{R}^d)$  be a bump function with  $\text{supp } h \subseteq B_\delta(x)$  and  $h(x) = 1$ . Then

$$\sum_{i=1}^N d_i \lambda_i h = \sum_{i=1}^N d_i [h(g(x_i)) - h(x_i)] = -d_k = 0,$$

Now consider  $X_{\text{new}} = X \setminus \{x_k\}$ . If this set is not empty, then we can repeat the above argument and use that  $X_{\text{new}}$  does not contain a fixed point or a entire periodic orbit and conclude that another coefficient  $d_i$  must be zero. Thus, we can show that all coefficients  $d_i = 0$ . The collocation matrix  $A$  with  $a_{ij} = \lambda_i^x \lambda_j^y \Phi(x, y) = \langle \lambda_i, \lambda_j \rangle_{H^*}$  is positive definite, since for  $\alpha \in \mathbb{R}^N$  we have

$$\alpha^T A \alpha = \sum_{i,j=1}^N \alpha_i \alpha_j a_{ij} = \left\| \sum_{i=1}^N \alpha_i \lambda_i \right\|_{H^*}^2 \geq 0$$

and it is zero if and only if  $\alpha = 0$  due to the linear independence of the  $\lambda_i$ .  $\square$

We set  $r_i = -1$  for all  $i = 1, \dots, N$ . Then the solution (8) is given by

$$v(x) = \sum_{j=1}^N \alpha_j [\phi(\|x - g(x_j)\|_2) - \phi(\|x - x_j\|_2)], \quad (10)$$

where  $\alpha \in \mathbb{R}^N$  is the solution to the linear system of equation

$$A\alpha = r,$$

with

$$\begin{aligned} a_{ij} &= \lambda_i^x [\phi(\|x - g(x_j)\|_2) - \phi(\|x - x_j\|_2)] \\ &= \phi(\|g(x_i) - g(x_j)\|_2) - \phi(\|x_i - g(x_j)\|_2) - \phi(\|g(x_i) - x_j\|_2) \\ &\quad + \phi(\|x_i - x_j\|_2). \end{aligned} \tag{11}$$

Note that

$$\begin{aligned} \Delta v(x) &= \sum_{j=1}^N \alpha_j [\phi(\|g(x) - g(x_j)\|_2) - \phi(\|x - g(x_j)\|_2) \\ &\quad - \phi(\|g(x) - x_j\|_2) + \phi(\|x - x_j\|_2)]. \end{aligned} \tag{12}$$

Since  $v$  interpolates the data, we have  $\Delta v(x_i) = r_i = -1$  at all collocation points. For other points sufficiently far from the chain-recurrent set, we expect  $\Delta v(x)$  to be close to  $-1$ , although no error estimates are available as described above. If  $x$  is in the chain-recurrent set, however, we expect  $\Delta v(x)$  to be close to 0. Thus, the set of points

$$\{x \in \mathbb{R}^d : \Delta v(x) \geq \gamma\}$$

with a threshold  $\gamma \in (-1, 0]$ , usually close to 0, can be expected to give some idea of the location of the chain-recurrent set. This method will be applied to examples in Section 5.

**4. Minimization problem.** In the previous section we have considered an equation for  $\Delta V(x)$ , which cannot have a solution for all points  $x$  in the chain-recurrent set.

In this section we will consider the inequality  $\Delta V(x) \leq 0$  instead of an equation for  $\Delta V(x)$ . Recall that this is the condition which defines a CLF candidate. The advantages compared to the method discussed in the previous section are that we know that a solution exists, and we can thus prove convergence in some cases. We will consider two methods: for the first one we only require minimal information on the chain-recurrent set and in the second case no information at all. The disadvantage of the methods in this section is that instead of solving a system of linear equations, we will now solve a quadratic programming problem, which is computationally a more demanding problem.

Let us describe the two approaches in more detail: the first one combines equality and inequality constraints and requires minimal information about the chain-recurrent set. More exactly, we need to know at least one point  $x_0$  which is not in the chain-recurrent set and will set  $\Delta V(x_0) = -1$ , while we require  $\Delta V(x) \leq 0$  for all other points. If there exists a CLF candidate  $W$  in our solution space for the system, then such a function  $V$  exists. Indeed, noting that  $\Delta W(x_0) < 0$ , as  $x_0$  is not in the chain-recurrent set, the function  $V(x) = c_0 W(x)$  with  $c_0 = -\frac{1}{\Delta W(x_0)} > 0$  satisfies the assumptions above.

We discretize the problem by choosing a set of pairwise distinct points  $X = \{x_0, x_1, \dots, x_N\}$ , such that there are no fixed points or entire periodic orbits of (1) in  $X$ , and we consider the following minimization problem, which can be solved by quadratic programming: for  $v \in H$

$$\left\{ \begin{array}{ll} \text{minimize} & \|v\|_H \\ \text{subject to} & \Delta v(x_0) = -1, \\ & \Delta v(x_i) \leq 0, i = 1, \dots, N \end{array} \right.$$

where  $H$  is a suitable Hilbert space. Note that if we only consider equality constraints, this reduces to the method of the previous section.

The second approach goes further and only considers inequality constraints of the form  $\Delta V(x) \leq 0$ . However, the norm-minimal solution of this problem is  $V \equiv 0$ . In order to obtain a nontrivial CLF candidate, which has a strictly negative orbital derivative in a large area, we minimize  $\|v\|_H^2 + \int_{\Omega} \Delta v(x) dx$ , thus rewarding strict negativity of  $\Delta v(x)$ . The discretized problem can again be solved by quadratic programming.

**4.1. Equality and inequality constraints.** In this section we adapt the theory from [18] to compute CLF candidates for discrete-time systems.

Let  $\Omega, S \neq \emptyset$  be bounded domains in  $\mathbb{R}^d$ , such that  $S$  has a Lipschitz boundary and  $\Omega, g(\Omega) \subseteq S$ . Consider a reproducing kernel Hilbert space  $H$  with inner product  $\langle \cdot, \cdot \rangle_H$ , norm  $\|\cdot\|_H$  and kernel  $\Phi: \mathbb{R}^d \times \mathbb{R}^d \rightarrow \mathbb{R}$  as described above, which is norm-equivalent to  $H^\sigma(S)$  where  $\sigma > d/2$ .

Fix a set of pairwise distinct collocation points  $X = \{x_0, x_1, \dots, x_N\} \subseteq \Omega$ , which does not contain any fixed points or entire periodic orbits of (1). Furthermore, we assume that  $x_0$  is not in the chain-recurrent set. We will impose an equality constraint on the single point  $x_0$  and inequality constraints for the other points in  $X$ . Note that the theory equally holds if we impose equality constraints on more points in  $X$  than  $x_0$  if none of them is in the chain-recurrent set.

We consider the problem: for  $v \in H$

$$\begin{cases} \text{minimize} & \|v\|_H \\ \text{subject to} & \Delta v(x_0) = -1, \\ & \Delta v(x_i) \leq 0, i = 1, \dots, N \end{cases} \quad (13)$$

In [18] the theory for general  $\lambda_i \in H^*$  is developed and all results hold when considering  $\lambda_i = \delta_{x_i} \circ \Delta$ . In particular, [18] shows that the problem (13) has a unique solution, which is of the form

$$v(x) = \sum_{j=0}^N \alpha_j (\delta_{x_j} \circ \Delta)^y \Phi(x, y), \quad (14)$$

where the coefficients  $\alpha = (\alpha_j)_{j=0,\dots,N}$  are the unique solution of the problem: for  $\alpha \in \mathbb{R}^{N+1}$

$$\begin{cases} \text{minimize} & \alpha^T A \alpha \\ \text{subject to} & A_{=} \alpha = -1 \\ \text{and} & A_{\leq} \alpha \leq 0 \in \mathbb{R}^N. \end{cases} \quad (15)$$

Here, the inequality is to be read componentwise, the matrix elements  $a_{ij}$  are defined by

$$a_{ij} = \lambda_i^x \lambda_j^y \Phi(x, y)$$

and the matrices by

$$\begin{aligned} A &= (a_{ij})_{i,j=0,\dots,N} \in \mathbb{R}^{(N+1) \times (N+1)} = \begin{pmatrix} A_{=} \\ A_{\leq} \end{pmatrix}, \\ A_{=} &= (a_{0j})_{j=0,\dots,N} \in \mathbb{R}^{1 \times (N+1)}, \\ A_{\leq} &= (a_{ij})_{i=1,\dots,N, j=0,\dots,N} \in \mathbb{R}^{N \times (N+1)}. \end{aligned}$$

Note that the explicit formulas for the matrix  $A$  and its sub-matrices  $A_{=}$  and  $A_{\leq}$  are the same as in (11). The problem (15) is a quadratic programming problem.

The explicit formulas for  $v$  and  $\Delta v$  are the same as in (10) and (12), when starting the sum at 0 rather than 1.

**4.2. Inequality constraints.** In this section we adapt the theory from [19] to compute CLF candidates for discrete-time systems.

Let  $\Omega, S \neq \emptyset$  be bounded domains in  $\mathbb{R}^d$ , such that  $S$  has a Lipschitz boundary and  $\Omega, g(\Omega) \subseteq S$ . While [19] considers the theory for general linear differential operators  $L : H^\sigma(\Omega) \rightarrow H^{\sigma-m}(\Omega)$  of order  $m$ , we have a linear operator  $\Delta : H^\sigma(S) \rightarrow H^\sigma(\Omega)$ ,  $\Omega \subseteq S$ , that is not a differential operator, i.e.  $m = 0$ . Note in particular that  $(v \circ g) \in H^\sigma(\Omega)$  by our assumptions on  $v$  and  $g$  (see below).

We are concerned with the problem: for  $v \in H$

$$\begin{cases} \text{minimize} & \|v\|_H^2 + \int_{\Omega} \Delta v(x) dx \\ \text{subject to} & \Delta v(x) \leq 0, \forall x \in \Omega \end{cases} \quad (16)$$

Let us first consider a discretized version. We choose a set of pairwise distinct collocation points  $X = \{x_1, \dots, x_N\} \subseteq \Omega$ , not containing any fixed point or entire periodic orbit of (1). Furthermore, we fix  $w_i > 0$  for all  $i = 1, \dots, N$ . Denote by  $H$  a reproducing kernel Hilbert space with inner product  $\langle \cdot, \cdot \rangle_H$ , norm  $\|\cdot\|_H$  and kernel  $\Phi$  as above, which is norm-equivalent to  $H^\sigma(S)$  with  $\sigma > d/2 + 1$ , i.e. we have in particular  $H^\sigma(S) \subseteq C^0(S)$ . Note that  $\lambda_i = \delta_{x_i} \circ \Delta \in H^*$  and the  $\lambda_i$  are linearly independent by Lemma 3.1.

We assume that  $g$  in (1) is in  $C^{[\sigma]}(\mathbb{R}^d)$ . Consider the problem: for  $v \in H$

$$\begin{cases} \text{minimize} & \|v\|_H^2 + \sum_{i=1}^N \Delta v(x_i) w_i \\ \text{subject to} & \Delta v(x_i) \leq 0, \quad i = 1, \dots, N \end{cases} \quad (17)$$

Using the same arguments as in Section 3.1 of [19] with  $\lambda_i = \delta_{x_i} \circ \Delta \in H^*$ , which are linearly independent by Lemma 3.1, we can conclude that (17) has a unique solution which can be determined by solving a quadratic programming problem.

In particular, the solution  $v$  of (17) is of the form

$$v(x) = \sum_{j=1}^N \alpha_j (\delta_{x_j} \circ \Delta)^y \Phi(x, y), \quad (18)$$

where the coefficient  $\alpha = (\alpha_1, \dots, \alpha_N) \in \mathbb{R}^N$  is the unique solution of the problem: for  $\alpha \in \mathbb{R}^N$

$$\begin{cases} \text{minimize} & \alpha^T A \alpha + c^T \alpha \\ \text{subject to} & A \alpha \leq 0 \in \mathbb{R}^N. \end{cases} \quad (19)$$

Here, the inequality is to be read componentwise and  $c = (c_j)_{j=1, \dots, N}$  is defined by  $c_j = \sum_{i=1}^N A_{ij} w_i$  for  $j = 1, \dots, N$ . Moreover,  $A = (a_{ij})_{i,j=1, \dots, N}$  is defined by

$$a_{ij} = (\delta_{x_i} \circ \Delta)^x (\delta_{x_j} \circ \Delta)^y \Phi(x, y), \quad i, j = 1, \dots, N.$$

Note that the explicit formula for the matrix  $A$  is the same as in (11). The problem (19) is a quadratic programming problem. The explicit formulas for  $v$  and  $\Delta v$  are the same as in (10) and (12).

Now consider the original non-discretized problem (16). We will show that the minimization problem (16) has a unique solution  $v$ . Moreover,  $v$  is the limit of minimizers of the corresponding discretized versions (17), which in turn can be found as solutions of quadratic programming problems.

The relation to the discretized version is that we subdivide the set  $\Omega$  into finitely many, pairwise disjoint measurable sets  $\Omega_i \subseteq \Omega$ ,  $i = 1, \dots, N$ , with  $\bigcup_{i=1}^N \Omega_i = \Omega$ .

and  $w_i := |\Omega_i| > 0$ . Furthermore, we choose points  $x_i \in \Omega_i$  and define  $\lambda_i \in H^*$  by  $\lambda_i(v) = \Delta v(x_i)$  for  $i = 1, \dots, N$ . The connection between (16) and (17) is that the second term in the cost function in (17) converges to the integral  $\int_{\Omega} \Delta v(x) dx$  as  $n \rightarrow \infty$ .

We consider problem (16) and show that it has a unique solution, which is the limit of the solutions of the discretized problem. In the theorem, one assumption is that a function exists, which satisfies the constraints of a CLF candidate. Note that the constant function  $V_0 \equiv 0$  trivially satisfies these constraints. A proof of the theorem is given in the appendix.

**Theorem 4.1.** *Let  $\Omega, S \neq \emptyset$  be bounded domains in  $\mathbb{R}^d$ , such that  $S$  has a Lipschitz boundary and  $\Omega, g(\Omega) \subseteq S$ . Define  $H \cong H^{\sigma}(S)$  to be the RKHS with kernel  $\Phi(x, y) = \psi_{l,k}(c\|x - y\|_2)$  restricted to  $S^2$ , where  $c > 0$  and  $\psi_{l,k}$  denotes the Wendland function with  $k \in \mathbb{N}$ ,  $l = \lfloor \frac{d}{2} \rfloor + k + 1$ . Here  $\sigma = k + \frac{d+1}{2} > d/2 + 1$ . Let  $g \in C^{[\sigma]}(\mathbb{R}^d)$ .*

*Consider the problem: for  $v \in H$*

$$\begin{cases} \text{minimize} & \|v\|_H^2 + \int_{\Omega} \Delta v(x) dx \\ \text{subject to} & \Delta v(x) \leq 0 \text{ for all } x \in \Omega. \end{cases} \quad (20)$$

*and the sequence of optimization problems:*

*Let  $\Omega_1^n, \dots, \Omega_{N_n}^n \subseteq \Omega$ ,  $n \in \mathbb{N}$ , be measurable sets with*

- $|\Omega_i^n| > 0$  for all  $i = 1, \dots, N_n$ ,
- $\bigcup_{i=1}^{N_n} \Omega_i^n = \Omega$  for all  $n \in \mathbb{N}$ ,
- $\Omega_i^n \cap \Omega_j^n = \emptyset$  for all  $i \neq j$  and all  $n \in \mathbb{N}$ ,
- $d_n := \max_{i=1, \dots, N_n} d_i^n \rightarrow 0$  as  $n \rightarrow \infty$ , where  $d_i^n = \text{diam } \Omega_i^n = \sup_{x, y \in \Omega_i^n} \|x - y\|_2$ .

*For  $n \in \mathbb{N}$  and  $i = 1, \dots, N_n$  let  $x_i^n \in \Omega_i^n$  be such that  $X^n := \{x_1^n, x_2^n, \dots, x_{N_n}^n\}$  does not contain any fixed point or entire periodic orbit of (1). For each fixed  $n \in \mathbb{N}$  let  $v_n$  be the solution to: for  $v \in H$*

$$\begin{cases} \text{minimize} & \|v\|_H^2 + \sum_{i=1}^{N_n} \Delta v(x_i^n) |\Omega_i^n| \\ \text{subject to} & \Delta v(x_i^n) \leq 0, \quad i = 1, \dots, N_n. \end{cases} \quad (21)$$

*Then the optimization problem (20) has a unique solution and the solutions  $v_n$  to the optimization problems (21) converge strongly in  $H$  to  $v$  as  $n \rightarrow \infty$ .*

**Remark 1.** One might be tempted to consider a seemingly more general version of (20): for  $v \in H$

$$\begin{cases} \text{minimize} & \|v\|_H^2 + R \int_{\Omega} \Delta v(x) dx \\ \text{subject to} & \Delta v(x) \leq 0 \text{ for all } x \in \Omega \end{cases} \quad (22)$$

with a parameter  $R > 0$ . However, this problem is not more general. If  $v$  is the unique minimizer of (20), then  $w = Rv$  is the unique minimizer of (22). Assume for a contradiction that  $w = Rv$  is not the minimizer of (22). Then there exists  $u \in H$  such that

$$\|u\|_H^2 + R \int_{\Omega} \Delta u(x) dx < \|w\|_H^2 + R \int_{\Omega} \Delta w(x) dx = R^2 \left( \|v\|_H^2 + \int_{\Omega} \Delta v(x) dx \right)$$

and we have

$$\|\tilde{u}\|_H^2 + \int_{\Omega} \Delta \tilde{u}(x) dx < \|v\|_H^2 + \int_{\Omega} \Delta v(x) dx$$

with  $\tilde{u} = R^{-1}u$ . Since  $\tilde{u}$  fulfills the constraints of (20)  $v$  cannot be the minimizer.

In the examples below we will see that the absolute values of the CLF candidates and their orbital derivatives, computed with this method, are very small in comparison to the other two methods. This is to be expected due to the objective function of the minimization problem. However, one can obtain a multiple  $w = Rv$  with larger absolute values by introducing a factor  $R$  as discussed in Remark 1 with identical chain-recurrent set.

Example	$N$	$\alpha_{\text{Hexa-basis}}$	#-evaluation	$x_{\min}$	$x_{\max}$	$y_{\min}$	$y_{\max}$	$z_{\min}$	$z_{\max}$
(24)	3,584	0.072	1,779,556	-2	2	-2	2		
(25)	10,108	0.03	2,003,001	-2	2	-1	1		
(26)	1,440	0.05	1,334,000	-1.5	1.5	-0.5	0.5		
(27)	5,520	0.025	1,334,000	-1.5	1.5	-0.5	0.5		
(28)	2,900	0.08	1,779,556	-2	2	-2	2		
(29)	5,301	0.07	1,030,301	-0.2	0.9	-0.2	0.9	-0.2	0.9

TABLE 1. Collocation points  $X$  for the examples. We have used  $N$  collocation points in a hexagonal grid with parameter  $\alpha_{\text{Hexa-basis}}$  within a rectangle  $(x, y) \in [x_{\min}, x_{\max}] \times [y_{\min}, y_{\max}]$  or  $(x, y, z) \in [x_{\min}, x_{\max}] \times [y_{\min}, y_{\max}] \times [z_{\min}, z_{\max}]$  for the three-dimensional example (29). The number of evaluation points is also displayed.

System	$\gamma$ for each method		
	$\Delta v(x) = -1$	equality-inequality	inequality
(24)	-0.1	$-10^{-5}$	0
(25)	-0.2	$-10^{-5}$	$-10^{-4}$
(26)	-0.1	0	$-10^{-2}$
(27)	-0.1	0	0
(28)	-0.1	0	0
(29)	-0.1	0	0

TABLE 2. The value of the parameter  $\gamma \leq 0$ , close to 0, for all examples. The chain-recurrent set is approximated by the set  $(\Delta v)^{-1}([\gamma, \infty))$ .

**5. Examples.** We apply all the previous methods to five two-dimensional systems and one three-dimensional system, starting from relatively simple dynamics to more complicated attractors.

For all examples we have used the Wendland function  $\psi_{6,4}(r) = (1 - r)_+^6(35r^2 + 18r + 3)$  and the kernel  $\Phi(x, y) = \psi_{6,4}(c\|x - y\|_2)$  with  $c = 1$  when solving  $\Delta v(x, y) = -1$  (Section 3), with  $c = 0.1$  for the equality and inequality constraints (Section 4.1), and with  $c = 0.4$  for the inequality constraints only (Section 4.2). The different  $c$  were fixed for the different cases using trial-and-error. Lower  $c$  correspond to larger supports of the radial basis functions, which improves the accuracy in the approximation at the cost of larger condition numbers of the collocation matrices. For all planar examples, we have used the extra point  $x_0 = (0.5, 0)$  for the equality constraint (see Section 4.1) and for the three-dimensional example (29) we enforced the equality at  $x_0 = (0.4, 0.4, 0)$ .

In Table 1 we specify the collocation points used: they are the intersection of the specified rectangle with the (shifted) hexagonal grid (23) with fineness-parameter

$\alpha_{\text{Hexa-basis}} \in \mathbb{R}^+$ , see [27], where it is shown that this grid gives the optimum fill distance for a given density of grid points.

$$\begin{aligned} \alpha_{\text{Hexa-basis}} & \left\{ \frac{\omega_d}{2} + \sum_{k=1}^d i_k \omega_k : i_k \in \mathbb{Z} \right\}, \quad \text{where} \\ \omega_1 & = (2\varepsilon_1, 0, 0, \dots, 0) \\ \omega_2 & = (\varepsilon_1, 3\varepsilon_2, 0, \dots, 0) \\ & \vdots \quad \vdots \\ \omega_d & = (\varepsilon_1, \varepsilon_2, \varepsilon_3, \dots, (d+1)\varepsilon_d) \text{ and} \\ \varepsilon_k & = \sqrt{\frac{1}{2k(k+1)}}, \quad k \in \mathbb{N}. \end{aligned} \quad (23)$$

We check the collocation points in  $X$  for fixed points and entire periodic orbits, which must to be removed from  $X$ , for otherwise the collocation matrix is singular. Further, the evaluation points are the points of a Cartesian grid where we evaluated  $v$  and  $\Delta v$  to approximate the chain-recurrent set and plot the functions. Note that only in the case of the method from Section 4.2 using inequalities we know that a sufficiently dense collocation grid will deliver good results, cf. Theorem 4.1. For the other methods this is a hypothesis.

For the first method, if the original problem had a solution, then error estimates are available in terms of the fill distance, which show that the error between true solution and approximation is bounded by the fill distance of the collocation points. However, in our case, the original problem does not have a solution for points in the chain-recurrent set, hence, this argumentation does not hold. Nonetheless, numerical experiments show that in the continuous-time case also here a denser collocation grid provides better results.

Our approximation of the chain-recurrent set is the set  $(\Delta v)^{-1}([\gamma, \infty))$ , where  $\gamma \leq 0$  is close to zero. Table 2 displays the values of  $\gamma$  used in the examples. In each case the value for  $\gamma$  was fixed using some experimenting what values gave the best results. Note that for the last two methods,  $\gamma = 0$  is the natural choice.

**5.1. Linear system.** We consider the system (1) with

$$g(x, y) = \begin{pmatrix} \frac{1}{2}x \\ \frac{1}{3}y \end{pmatrix}. \quad (24)$$

The origin is an asymptotically stable fixed point, which is the entire chain-recurrent set. Hence, a CLF should have negative orbital derivative everywhere except for the origin where it should be 0. The origin should be a minimum of the CLF.

The results are shown in Figure 1 for solving  $\Delta v(x, y) = -1$  (Section 3), in Figure 2 for the equality and inequality constraints (Section 4.1), and in Figure 3 for the inequality constraints (Section 4.2). All three methods manage to find a good approximation of the chain-recurrent set.

**5.2. Saddle point.** We consider the system (1) with

$$g(x, y) = \begin{pmatrix} x^3 \\ 2y \end{pmatrix}. \quad (25)$$

The origin is a saddle point with stable manifold in  $x$ -direction and unstable manifold in  $y$ -direction, while  $(\pm 1, 0)$  are unstable fixed points with a 2-dimensional

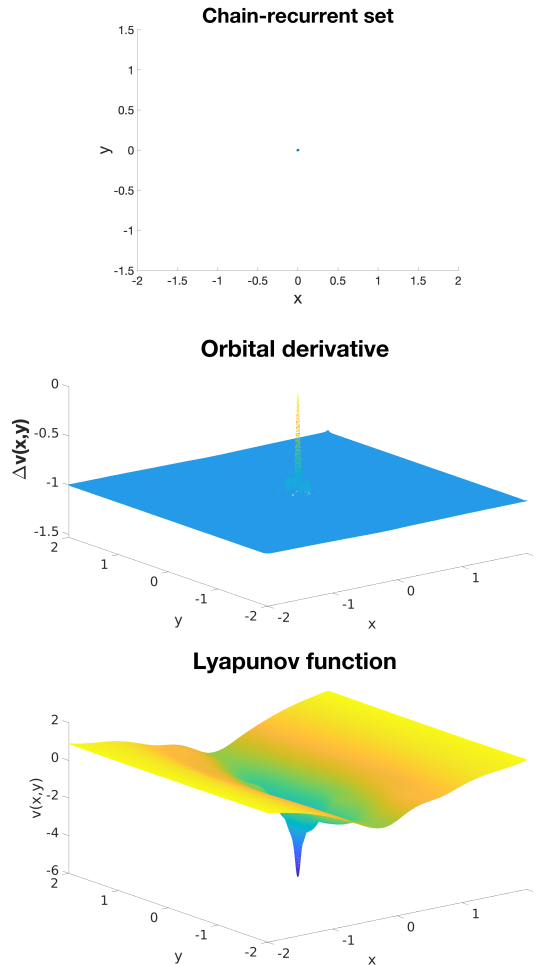


FIGURE 1. Example (24) with solving  $\Delta v(x, y) = -1$ . Chain-recurrent set (top) approximated by the set  $\{(x, y) \mid \Delta v(x, y) \geq \gamma\}$ , see Table 2, and the orbital derivative (middle)  $\Delta v(x, y)$  of the constructed complete Lyapunov function  $v$ .  $\Delta v$  is approximately zero on the chain-recurrent set (origin) and negative everywhere else. Bottom: Constructed complete Lyapunov function  $v(x, y)$ , which has a minimum at the origin.

unstable manifold. The chain-recurrent set is thus  $\{(0, 0)\} \cup \{\pm 1, 0\}$  and a CLF should have zero orbital derivative at these three fixed points and negative orbital derivative elsewhere. Moreover, a CLF should have a saddle point at  $\{(0, 0)\}$ , which is a minimum along the  $x$ -axis and a maximum along the  $y$ -axis, as well as a local maximum at  $(\pm 1, 0)$ . The second and third methods are able to approximate the chain-recurrent set much better than the first one.

The results are shown in Figure 4 for solving  $\Delta v(x, y) = -1$  (Section 3), in Figure 5 for the equality and inequality constraints (Section 4.1), and in Figure 6 for the inequality constraints (Section 4.2).

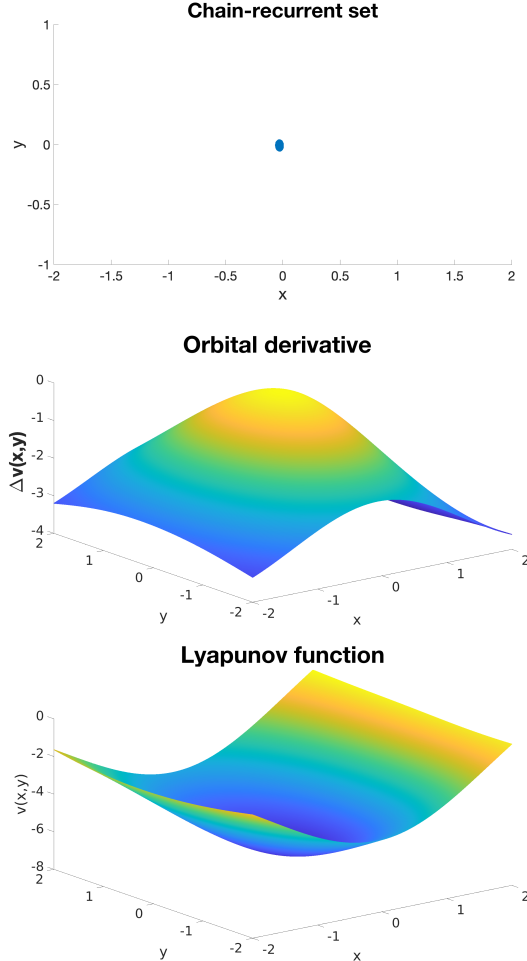


FIGURE 2. Example (24) with equality and inequality constraints. Chain-recurrent set (top) approximated by the set  $\{(x, y) \mid \Delta v(x, y) \geq \gamma\}$ , see Table 2, and the orbital derivative  $\Delta v(x, y)$  of the constructed complete Lyapunov function  $v$  (middle). Again, the orbital derivative  $\Delta v$  is correctly approximated being zero on the chain-recurrent set (origin) and negative everywhere else. Bottom: Constructed complete Lyapunov function  $v(x, y)$ , which has a minimum at the origin. The point with equality constraint was  $(0.5, 0)$ .

**5.3. Hénon map.** We consider the system (1) with

$$g(x, y) = \begin{pmatrix} 1 - ax^2 + y \\ bx \end{pmatrix} \quad (26)$$

and the classical parameters  $a = 1.4$  and  $b = 0.3$ . For these parameters, there exists an attractor  $A$ , which is the chain-recurrent set. A CLF should have zero orbital derivative on  $A$  and negative orbital derivative elsewhere. Moreover, it should attain a local minimum at  $A$  with the same value, as this is a chain-transitive component.

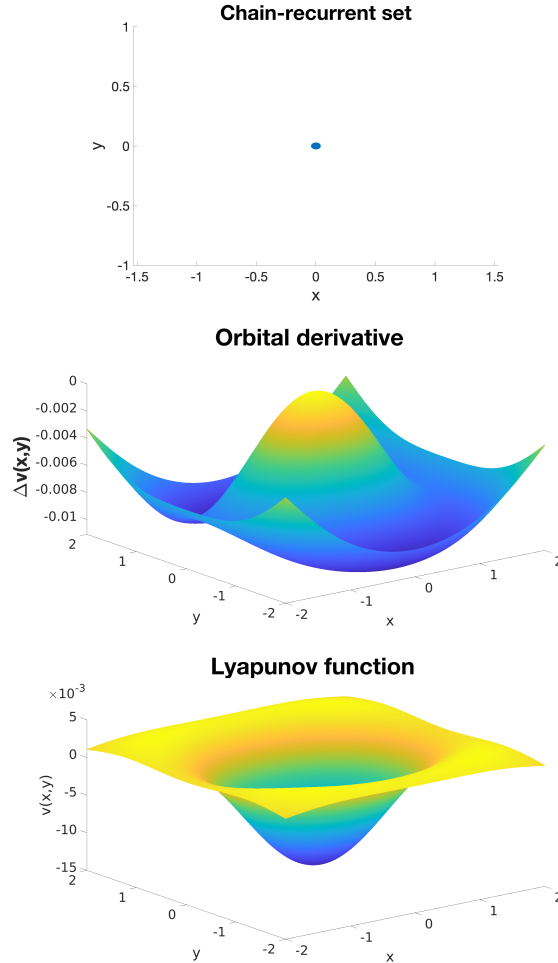


FIGURE 3. Example (24) with inequality constraints. Chain recurrent set (top) approximated by the set  $\{(x, y) \mid \Delta v(x, y) \geq \gamma\}$ , see Table 2, and the orbital derivative  $\Delta v(x, y)$  of the constructed complete Lyapunov function  $v$  (middle).  $\Delta v$  is approximately zero on the chain-recurrent set (origin) and negative everywhere else. Bottom: The constructed complete Lyapunov function  $v(x, y)$ , which has a minimum at the origin.

The results are shown in Figure 7 for solving  $\Delta v(x, y) = -1$  (Section 3), in Figure 8 for the equality and inequality constraints (Section 4.1), and in Figure 9 for the inequality constraints (Section 4.2). While the first method delivers poor results, both methods with constraints clearly show the Hénon attractor.

**5.4. Time-reversed Hénon map.** Note that attractors can be found by simulating forward trajectories. It is more difficult to find repellers. However, our methods are equally capable of localizing repellers, which are equally important for the chain-recurrent set and are characterized as local maxima, rather than minima in case of attractors, of a CLF. Note, that although the connection between CLFs of the

Hénon map and the time-reversed Hénon map is trivial, we cannot expect our methods to compute such functions to be invariant in the same sense. This is because the methods are only considering a subset of the whole phase space and solution trajectories can and will jump out of this subset.

We consider the system (1) with

$$g(x, y) = \begin{pmatrix} \frac{y}{b} \\ x - 1 + \frac{a}{b^2} y^2 \end{pmatrix} \quad (27)$$

and the classical parameters  $a = 1.4$  and  $b = 0.3$ . This is the inverse of the map in (26) and thus system (26) with inverse time. Hence, the Hénon attractor  $A$  of (26) is a repeller for (27). A CLF should have zero orbital derivative on  $A$  and negative orbital derivative elsewhere. Moreover, it should attain a local maximum at  $A$  with the same value, as this is a chain-transitive component.

The results are shown in Figure 10 for solving  $\Delta v(x, y) = -1$  (Section 3), in Figure 11 for the equality and inequality constraints (Section 4.1), and in Figure 12 for the inequality constraints (Section 4.2). While the first method delivers slightly better results than for the attractor in the previous example, both methods with constraints are still superior and clearly show the Hénon repeller.

**5.5. Duffing map.** We consider the system (1) with

$$g(x, y) = \begin{pmatrix} y \\ -bx + ay - y^3 \end{pmatrix} \quad (28)$$

and the classical parameters  $a = 2.75$  and  $b = 0.2$ . For these parameters, there exists an attractor  $A$ , which is the chain-recurrent set. A CLF should have zero orbital derivative on  $A$  and negative orbital derivative elsewhere. Moreover, it should attain a local minimum at  $A$  with the same value, as this is a chain-transitive component.

The results are shown in Figure 13 for solving  $\Delta v(x, y) = -1$  (Section 3), in Figure 14 for the equality and inequality constraints (Section 4.1), and in Figure 15 for the inequality constraints (Section 4.2). The methods with constraints clearly show the attractor, while the first method's results are not as clear.

**5.6. Three-dimensional Hénon map.** We consider the three-dimensional version of the Hénon map, described e.g. in [21]. We consider the system (1) with

$$g(x, y, z) = \begin{pmatrix} y \\ z \\ M_1 + Bx + M_2 y - z^2 \end{pmatrix} \quad (29)$$

and the parameters  $M_1 = 0$ ,  $B = 0.7$  and  $M_2 = 0.85$ . For these parameters, there exists an attractor  $A$ , which is the chain-recurrent set. A CLF should have zero orbital derivative on  $A$  and negative orbital derivative elsewhere. Moreover, it should attain a local minimum at  $A$  with the same value, as this is a chain-transitive component.

For this three-dimensional example the figures show the approximation of the chain-recurrent set  $\{(x, y, z) \mid \Delta v(x, y, z) \geq \gamma\}$  and projections of this set on planes. Figure 16 shows the results for solving  $\Delta v(x, y, z) = -1$  (Section 3), Figure 17 for the equality and inequality constraints (Section 4.1), and Figure 18 for the inequality constraints (Section 4.2). For this example, the first and last method show the best results, while the second method, using equality and inequality constraints, delivers the worst results.

**6. Discussion.** We have presented three methods to compute a complete Lyapunov function candidate (CLF) for a general discrete-time dynamical system. The first method approximates the equation  $\Delta V(x) = -1$  using meshfree collocation by solving a system of linear equations. The equation does not have a solution on the chain-recurrent set, and hence no error estimates are available. Nevertheless, for the simpler examples this method produces reasonable approximations of the chain-recurrent set.

The other two methods use quadratic optimization with equality-inequality constraints or inequality constraints, respectively. Generally, the optimization methods with equality-inequality and inequality constraints are computationally much more demanding than solving a system of linear equations and do not allow for as many collocation points. For the equality-inequality constraints, we need to identify one point outside the chain-recurrent set. This method gives in general inferior results. For the inequality constraints, no information about the chain-recurrent set is required, and we have shown that the solutions of the discretized problems converge to a complete Lyapunov function candidate. This method delivers the best results in the examples and should be considered superior to the others for computing CLF candidates for discrete-time systems. Additionally, for this method we were able to develop theory that asserts that the solutions to the discretized problems converge to the solution of the continuous problem, and that its solution is a non-trivial CLF candidate with  $\gamma = 0$ .

## REFERENCES

- [1] E. Akin, *The General Topology of Dynamical Systems*, American Mathematical Society, 1993.
- [2] C. Argáez, P. Giesl and S. Hafstein, Analysing dynamical systems towards computing complete Lyapunov functions, In *Proceedings of the 7th International Conference on Simulation and Modeling Methodologies, Technologies and Applications, Madrid, Spain*, pages 323–330, 2017.
- [3] C. Argáez, P. Giesl and S. Hafstein, Computation of complete Lyapunov functions for three-dimensional systems, In *Proceedings of the 57rd IEEE Conference on Decision and Control (CDC)*, pages 4059–4064, 2018.
- [4] C. Argáez, P. Giesl and S. Hafstein, *Dynamical systems in theoretical perspective, Chapter Computational Approach for Complete Lyapunov Functions*, **248** (2018), 1–11. Springer, Springer Proceedings in Mathematics and Statistics.
- [5] C. Argáez, P. Giesl and S. Hafstein, Iterative construction of complete Lyapunov functions, In *Proceedings of the 8th International Conference on Simulation and Modeling Methodologies, Technologies and Applications*, (2018), 211–222.
- [6] N. Aronszajn, *Theory of reproducing kernels*, *Trans. Amer. Math. Soc.*, **68** (1950), 337–404.
- [7] J. Auslander, Generalized recurrence in dynamical systems, *Contributions to Differential Equations*, **3** (1964), 65–74.
- [8] H. Ban and W. D. Kalies, *A computational approach to Conley's decomposition theorem*, *J. Comput. Nonlinear Dynam.*, **1** (2006), 312–319.
- [9] P. Bernard and S. Suhr, *Lyapunov functions of closed cone fields: From Conley theory to time functions*, *Commun. Math. Phys.*, **359** (2018), 467–498.
- [10] J. Björnsson, P. Giesl, S. F. Hafstein and C. M. Kellett, *Computation of Lyapunov functions for systems with multiple attractors*, *Discrete Contin. Dyn. Syst.*, **35** (2015), 4019–4039.
- [11] S. C. Brenner and L. R. Scott, *The Mathematical Theory of Finite Element Methods*, Texts in Applied Mathematics. Springer New York, 2008.
- [12] H. Brezis, *Functional Analysis, Sobolev Spaces and Partial Differential Equations*, Springer, 2011.
- [13] C. Conley, *Isolated Invariant Sets and the Morse Index*, CBMS Regional Conference Series in Mathematics, 38. American Mathematical Society, 1978.

- [14] M. Dellnitz, G. Froyland and O. Junge, The algorithms behind GAIO – set oriented numerical methods for dynamical systems, *Ergodic theory, Analysis, and Efficient Simulation of Dynamical Systems*, (2001), 145–174, 805–807.
- [15] A. Fathi and P. Pageault, *Smoothing Lyapunov functions*, *Trans. Amer. Math. Soc.*, **371** (2019), 1677–1700.
- [16] J. Franks, *Generalizations of the Poincaré-Birkhoff theorem*, *Ann. of Math.*, **128** (1998), 139–151. Erratum: [arXiv:math/0410316](https://arxiv.org/abs/math/0410316).
- [17] P. Giesl, *Construction of Global Lyapunov Functions Using Radial Basis Functions*, Lecture Notes in Math. 1904, Springer, 2007.
- [18] P. Giesl, C. Argáez, S. Hafstein and H. Wendland, Construction of a complete Lyapunov function using quadratic programming, In *Proceedings of the 15th International Conference on Informatics in Control, Automation and Robotics*, **1** (2018), 560–568.
- [19] P. Giesl, C. Argáez, S. Hafstein and H. Wendland, Convergence of discretized minimization problems with applications to complete Lyapunov functions, submitted, 2020.
- [20] P. Giesl and H. Wendland, *Meshless collocation: Error estimates with application to dynamical systems*, *SIAM J. Numer. Anal.*, **45** (2007), 1723–1741.
- [21] S. V. Gonchenko, I. I. Ovsyannikov, C. Simó and D. Turaev, *Three-dimensional Hénon-like maps and wild Lorenz-like attractors*, *Internat. J. Bifur. Chaos Appl. Sci. Engrg.*, **15** (2005), 3493–3508.
- [22] A. Goulet, S. Harker, K. Mischaikow, W. D. Kalies and D. Kasti, *Efficient computation of Lyapunov functions for Morse decompositions*, *Discrete Contin. Dyn. Syst. Ser. B*, **20** (2015), 2418–2451.
- [23] M. Hurley, *Chain recurrence and attraction in non-compact spaces*, *Ergodic Theory Dynam. Systems*, **11** (1991), 709–729.
- [24] M. Hurley, *Noncompact chain recurrence and attraction*, *Proc. Amer. Math. Soc.*, **115** (1992), 1139–1148.
- [25] M. Hurley, *Chain recurrence, semiflows, and gradients*, *J. Dynam. Differential Equations*, **7** (1995), 437–456.
- [26] M. Hurley, *Lyapunov functions and attractors in arbitrary metric spaces*, *Proc. Amer. Math. Soc.*, **126** (1998), 245–256.
- [27] A. Iske, Perfect centre placement for radial basis function methods, Technical Report TUM-M9809, TU Munich, Germany, 1998.
- [28] W. D. Kalies, K. Mischaikow and R. C. A. M. VanderVorst, *An algorithmic approach to chain recurrence*, *Found. Comput. Math.*, **5** (2005), 409–449.
- [29] D. E. Norton, The fundamental theorem of dynamical systems, *Comment. Math. Univ. Carolin.*, **36** (1995), 585–597.
- [30] M. Patrão, Existence of complete Lyapunov functions for semiflows on separable metric spaces, *Far East J. Dyn. Syst.*, **17** (2011), 49–54.
- [31] C. Robinson, *Dynamical Systems: Stability, Symbolic Dynamics, and Chaos*, Studies in Advanced Mathematics. CRC Press, 2. edition, 1999.
- [32] S. Suhr and S. Hafstein, Smooth complete Lyapunov functions for ODEs, submitted, 2020.
- [33] H. Wendland, *Error estimates for interpolation by compactly supported radial basis functions of minimal degree*, *J. Approx. Theory*, **93** (1998), 258–272.
- [34] H. Wendland, *Scattered Data Approximation*, volume 17 of Cambridge Monographs on Applied and Computational Mathematics, Cambridge University Press, Cambridge, 2005.

**Appendix.** In the appendix we give the proof of Theorem 4.1, which follows the proof of [19, Theorem 4.1], but has several modifications for our case of discrete-time systems.

*Proof of Theorem 4.1.* The kernel  $\Phi: \mathbb{R}^d \times \mathbb{R}^d \rightarrow \mathbb{R}$  can be written as  $\Phi(x, y) = \phi(\|x - y\|_2)$  with  $\phi \in C^{2k}(\mathbb{R}_0^+)$ . Because  $\phi$  is continuous on the compact set  $\bar{S}$  and  $g(x), x \in S$  for  $x \in \Omega$ , there exists a constant  $C$  such that

$$\sup_{x \in \Omega} (2\phi(0) - 2\phi(\|g(x) - x\|_2)) \leq C^2.$$

Set  $w_{i,n} := |\Omega_i^n|$ ,  $\lambda_x := \delta_x \circ \Delta \in H^*$  for  $x \in \Omega$ , and  $\lambda_{i,n} := \lambda_{x_i^n}$  in the following, and denote by  $\lambda_x^y \Phi(\cdot, y) \in H$  and  $\lambda_{i,n}^y \Phi(\cdot, y) \in H$  the Riesz representers of  $\lambda_x$  and  $\lambda_{i,n}$  respectively.

Step 1. boundedness of  $(v_n)_{n \in \mathbb{N}}$  and weakly converging subsequence

We have, using (5),

$$\begin{aligned}\|\lambda_{i,n}^y \Phi(\cdot, y)\|_H^2 &= \lambda_{i,n}^x \lambda_{i,n}^y \Phi(x, y) \\ &= \Phi(g(x_i^n), g(x_i^n)) - \Phi(x_i^n, g(x_i^n)) - \Phi(g(x_i^n), x_i^n) + \Phi(x_i^n, x_i^n) \\ &= 2\phi(0) - 2\phi(\|g(x_i^n) - x_i^n\|_2) \\ &\leq C^2.\end{aligned}$$

We have, see e.g. [34, Theorem 16.7],

$$\begin{aligned}-\sum_{i=1}^{N_n} \lambda_{i,n}(v_n) w_{i,n} &= -\sum_{i=1}^{N_n} w_{i,n} \langle v_n, \lambda_{i,n}^y \Phi(\cdot, y) \rangle_H \\ &\leq |\Omega| \|v_n\|_H C \\ &\leq \frac{1}{2} (\|v_n\|_H^2 + |\Omega|^2 C^2), \text{ i.e.} \\ -|\Omega|^2 C^2 - \|v_n\|_H^2 &\leq 2 \sum_{i=1}^{N_n} \Delta v_n(x_i^n) w_{i,n}. \tag{30}\end{aligned}$$

Note that  $V_0 \equiv 0$  fulfills the constraints of (20) and (21). Using (30) as well as that  $v_n$  is the minimizer of (21) we have

$$\begin{aligned}-|\Omega|^2 C^2 + \|v_n\|_H^2 &\leq 2 \left( \|v_n\|_H^2 + \sum_{i=1}^{N_n} \Delta v_n(x_i^n) w_{i,n} \right) \\ &\leq 2 \left( \|V_0\|_H^2 + \sum_{i=1}^{N_n} \Delta V_0(x_i^n) w_{i,n} \right) \\ &= 0.\end{aligned}$$

Thus,

$$\|v_n\|_H \leq C_0 := |\Omega| C \tag{31}$$

is bounded for all  $n$ . Since bounded sets are relatively compact in the weak topology of  $H$  there is a weakly convergent subsequence of the  $v_n$ .

In the following we consider *any* weakly convergent subsequence of the  $v_n$  with weak limit  $v \in H$ , and denote the subsequence again by  $v_n$ . We show that any such subsequence converges strongly to the unique minimizer of problem (20), and we will show the strong convergence of the original sequence at the end of the proof.

Note that we have

$$\|v\|_H \leq \limsup_{n \rightarrow \infty} \|v_n\|_H \leq C_0. \tag{32}$$

Step 2.  $\Delta v(x) \leq 0$  for all  $x \in \Omega$

Now we use the kernel representation to show that the limit  $v \in H$  from Step 1 fulfills the constraint of (20), i.e. that  $\Delta v(x) \leq 0$  for all  $x \in \Omega$ .

First note that for every  $x \in \Omega$  we have with  $\lambda_x = \delta_x \circ \Delta$

$$|\Delta v(x) - \Delta v_n(x)| = |\lambda_x(v - v_n)| = \langle v - v_n, \lambda_x^y \Phi(\cdot, y) \rangle_H \longrightarrow 0 \tag{33}$$

as  $v_n$  converges weakly to  $v$ .

We can write the kernel as  $\Phi(x, y) = \Psi(x - y)$  with  $\Psi: \mathbb{R}^d \rightarrow \mathbb{R}$ . Since  $\sigma > d/2 + 1$  the Sobolev embedding theorem shows that  $H^\sigma(\mathbb{R}^d) \subseteq W_\infty^1(\mathbb{R}^d) \cap C^1(\mathbb{R}^d)$ . Hence, there is an  $M > 0$  such that  $\|\nabla \Psi(\xi)\|_2 \leq M$  for all  $\xi \in \mathbb{R}^d$ . Since  $g \in C^1(\mathbb{R}^d)$ , there is  $M_g > 0$  such that  $\|Dg(\xi)\|_2 \leq M_g$  for all  $\xi \in \overline{\text{co } S}$ .

For  $x, y \in \Omega$  there are  $\xi, \eta \in \mathbb{R}^d$  on the line segment between 0 and  $x - y$  such that

$$\begin{aligned}
& |\Delta v_n(y) - \Delta v_n(x)| \\
&= |v_n(g(y)) - v_n(y) - v_n(g(x)) + v_n(x)| \\
&= |\langle v_n(\cdot), \Phi(\cdot, g(y)) - \Phi(\cdot, y) - \Phi(\cdot, g(x)) + \Phi(\cdot, x) \rangle_H| \\
&\leq \|v_n\|_H (\|\Phi(\cdot, g(y)) - \Phi(\cdot, g(x))\|_H + \|\Phi(\cdot, y) - \Phi(\cdot, x)\|_H) \\
&\leq \|v_n\|_H [(\Phi(g(y), g(y)) + \Phi(g(x), g(x)) - 2\Phi(g(y), g(x)))^{1/2} \\
&\quad + (\Phi(y, y) + \Phi(x, x) - 2\Phi(y, x))^{1/2}] \\
&\leq \|v_n\|_H \left[ (2\Psi(0) - 2\Psi(g(y) - g(x)))^{1/2} + (2\Psi(0) - 2\Psi(y - x))^{1/2} \right] \\
&\leq \sqrt{2}\|v_n\|_H \left[ (\|\nabla \Psi(g(\xi))\|_2 \|Dg(\xi)\|_2 \|y - x\|_2)^{1/2} + (\|\nabla \Psi(\eta)\|_2 \|y - x\|_2)^{1/2} \right] \\
&\leq \sqrt{2M}C_0 \sqrt{1 + M_g} \|y - x\|_2^{1/2} \\
&\leq C_1 \|y - x\|_2^{1/2}
\end{aligned} \tag{34}$$

for all  $n \in \mathbb{N}$  by (31), denoting  $C_1 = \sqrt{2M}C_0 \sqrt{1 + M_g}$ .

We will now show that the fill distance  $h_{X^n, \Omega} = \sup_{x \in \Omega} \min_{j=1, \dots, N_n} \|x - x_j^n\|_2$  satisfies

$$\lim_{n \rightarrow \infty} h_{X^n, \Omega} = 0. \tag{35}$$

Fix  $n \in \mathbb{N}$ . For a point  $x \in \Omega$ , there is an  $i \in \{1, \dots, N_n\}$  with  $x \in \Omega_i^n$ . We have

$$\min_{j=1, \dots, N_n} \|x - x_j^n\|_2 \leq \|x - x_i^n\|_2 \leq \sup_{y, z \in \Omega_i^n} \|y - z\|_2 = d_i^n \leq d_n.$$

Hence, we also have

$$h_{X^n, \Omega} = \sup_{x \in \Omega} \min_{j=1, \dots, N_n} \|x - x_j^n\|_2 \leq d_n.$$

This shows the statement, since  $d_n \rightarrow 0$  as  $n \rightarrow \infty$ .

We will show that for all  $x \in \Omega$  we have  $\Delta v(x) \leq 0$ . We do this by fixing  $x \in \Omega$  and showing that for all  $\varepsilon > 0$  we have  $\Delta v(x) < \varepsilon$ . Fix  $\varepsilon > 0$ . By (33), there is  $N_1 \in \mathbb{N}$  such that for all  $n \geq N_1$  we have

$$|\Delta v_n(x) - \Delta v(x)| < \frac{\varepsilon}{2}. \tag{36}$$

By (35) there is  $N_2 \in \mathbb{N}$  such that for all  $n \geq N_2$  there exists  $x_i^n \in X^n$  with

$$\|x - x_i^n\|_2 < \frac{\varepsilon^2}{4C_1^2}. \tag{37}$$

For  $n \geq \max(N_1, N_2)$  we have by (36), (34) and (37) as well as  $\Delta v_n(x_i^n) \leq 0$ , see (17),

$$\begin{aligned}\Delta v(x) &\leq (\Delta v(x) - \Delta v_n(x)) + (\Delta v_n(x) - \Delta v_n(x_i^n)) + \Delta v_n(x_i^n) \\ &< \frac{\varepsilon}{2} + C_1 \frac{\varepsilon}{2C_1} + 0 = \varepsilon.\end{aligned}$$

Step 3. weakly converging subsequence is strongly converging

Since  $\Delta v(x) \leq 0$  holds for all  $x \in \Omega$ , as shown in Step 2,  $v$  satisfies the constraints of (17) and thus

$$\|v_n\|_H^2 + \sum_{i=1}^{N_n} \Delta v_n(x_i^n) w_{i,n} \leq \|v\|_H^2 + \sum_{i=1}^{N_n} \Delta v(x_i^n) w_{i,n} \quad (38)$$

since  $v_n$  is the minimizer.

We will show that for  $\varepsilon > 0$  there exists  $N_0$  such that

$$\left| \sum_{i=1}^{N_n} \Delta v_n(x_i^n) w_{i,n} - \sum_{i=1}^{N_n} \Delta v(x_i^n) w_{i,n} \right| < \varepsilon \quad (39)$$

for all  $n \geq N_0$ . This implies that the weakly converging subsequence  $(v_n)_{n \in \mathbb{N}}$  from Step 1 is actually strongly converging to  $v$ , because (38) and (39) together imply that  $\limsup_{n \rightarrow \infty} \|v_n\|_H \leq \|v\|_H$ , cf. e.g. [12, Prop. 3.32].

Now we show (39). Define  $\mu(v) := \int_{\Omega} \Delta v(x) dx$ . We have  $\mu \in H^*$  since  $H \cong H^\sigma(S)$  and for a constant  $C_{\text{emb}}$  independent of  $v$

$$\begin{aligned}|\mu(v)| &\leq \int_{\Omega} [v(g(x)) - v(x)] dx \\ &\leq 2|\Omega| \sup_{x \in S} |v(x)| \\ &\leq 2|\Omega| C_{\text{emb}} \|v\|_{H^\sigma(S)}\end{aligned}$$

by Theorem 1.4.6 in [11] because  $\sigma > d/2+1 > d/2$  and  $S$  has a Lipschitz boundary. Hence, we have, with  $\mu^y \Phi(\cdot, y) \in H$  as the Riesz representative of  $\mu \in H^*$ ,

$$\int_{\Omega} (\Delta v_n(x) - \Delta v(x)) dx = \langle v_n - v, \mu^y \Phi(\cdot, y) \rangle_H \longrightarrow 0$$

as  $n \rightarrow \infty$  since  $v_n$  converges weakly to  $v$  in  $H$ . Hence, there is  $N_1 \in \mathbb{N}$  such that for all  $n \geq N_1$  we have

$$\left| \int_{\Omega} (\Delta v_n(x) - \Delta v(x)) dx \right| < \varepsilon/3. \quad (40)$$

Then we have

$$\begin{aligned}
\left| \int_{\Omega} \Delta v_n(x) dx - \sum_{i=1}^{N_n} w_{i,n} \Delta v_n(x_i^n) \right| &= \left| \sum_{i=1}^{N_n} \int_{\Omega_i} \Delta v_n(x) dx - \sum_{i=1}^{N_n} \int_{\Omega_i} \Delta v_n(x_i^n) dx \right| \\
&\leq \sum_{i=1}^{N_n} \int_{\Omega_i} |\Delta v_n(x) - \Delta v_n(x_i^n)| dx \\
&\leq C_1 \sum_{j=1}^{N_n} \int_{\Omega_j} \|x - x_i^n\|^{1/2} dx \text{ by (34)} \\
&\leq C_1 \sum_{j=1}^{N_n} d_n^{1/2} \int_{\Omega_j} dx \\
&= C_1 d_n^{1/2} |\Omega|
\end{aligned} \tag{41}$$

Note that the same estimate holds for  $v$  instead of  $v_n$ , since (34) holds with the same constant by (32).

Since  $d_n \rightarrow 0$  as  $n \rightarrow \infty$  there is  $N_2 \in \mathbb{N}$  such that for all  $n \geq N_2$  we have  $d_n < \frac{\varepsilon^2}{9C_1^2|\Omega|^2}$ . For  $n \geq N_0 := \max(N_1, N_2)$  we have

$$\begin{aligned}
\left| \sum_{i=1}^{N_n} \Delta v_n(x_i^n) w_{i,n} - \sum_{i=1}^{N_n} \Delta v(x_i^n) w_{i,n} \right| &\leq \left| \sum_{i=1}^{N_n} \Delta v_n(x_i^n) w_{i,n} - \int_{\Omega} \Delta v_n(x) dx \right| \\
&\quad + \left| \int_{\Omega} \Delta v_n(x) dx - \int_{\Omega} \Delta v(x) dx \right| \\
&\quad + \left| \int_{\Omega} \Delta v(x) dx - \sum_{i=1}^{N_n} \Delta v(x_i^n) w_{i,n} \right| \\
&< \varepsilon
\end{aligned}$$

by (41) and (40), which shows (39).

#### Step 4. $v$ is unique minimizer

Finally, we seek to show that  $v$  is the unique minimizer. First, let us show that  $v$  is a minimizer. Assume that  $V \in H$  is any function satisfying the constraints of (20). For every  $n$ ,  $V$  also satisfies the constraints of the discrete problem, so we have

$$\|v_n\|_H^2 + \sum_{i=1}^{N_n} \Delta v_n(x_i^n) w_{i,n} \leq \|V\|_H^2 + \sum_{i=1}^{N_n} \Delta V(x_i^n) w_{i,n}$$

As  $n \rightarrow \infty$ , this becomes

$$\|v\|_H^2 + \int_{\Omega} \Delta v(x) dx \leq \|V\|_H^2 + \int_{\Omega} \Delta V(x) dx \tag{42}$$

as  $\|v_n\|_H \rightarrow \|v\|_H$  due to the strong convergence,  $\sum_{i=1}^{N_n} \Delta v_n(x_i^n) w_{i,n} \rightarrow \int_{\Omega} \Delta v(x) dx$  using (40) and (41) and  $\sum_{i=1}^{N_n} \Delta V(x_i^n) w_{i,n} \rightarrow \int_{\Omega} \Delta V(x) dx$  similar to (41). Equation (42) shows that  $v$  is a minimizer.

To show that there is not more than one minimizer, we first assume that  $s \in H$  is a minimizer and  $v \in H$  satisfies the constraints of (20) and show that

$$2\langle s, v - s \rangle_H + \int_{\Omega} \Delta(v - s)(x) dx \geq 0. \tag{43}$$

For this assume that  $2\langle s, v - s \rangle_H + \int_{\Omega} \Delta(v - s)(x) dx < 0$ . Let  $\alpha \in [0, 1]$ . Note that  $t = \alpha v + (1 - \alpha)s$  satisfies the constraints and we have

$$\begin{aligned} \|t\|_H^2 + \int_{\Omega} \Delta t(x) dx &= \|s + \alpha(v - s)\|_H^2 + \int_{\Omega} \Delta[s + \alpha(v - s)](x) dx \\ &= \|s\|_H^2 + 2\alpha\langle s, v - s \rangle_H + \alpha^2\|v - s\|_H^2 \\ &\quad + \int_{\Omega} \Delta s(x) dx + \alpha \int_{\Omega} \Delta(v - s)(x) dx \\ &< \|s\|_H^2 + \int_{\Omega} \Delta s(x) dx \end{aligned}$$

for a suitable  $\alpha > 0$ . This is a contradiction to  $s$  being a minimizer.

Now let  $s_1, s_2 \in H$  be minimizers. Then by (43) we have  $2\langle s_1, s_2 - s_1 \rangle_H + \int_{\Omega} \Delta(s_2 - s_1)(x) dx \geq 0$  and  $2\langle s_2, s_1 - s_2 \rangle_H + \int_{\Omega} \Delta(s_1 - s_2)(x) dx \geq 0$ .

This implies

$$\begin{aligned} 0 &\leq 2\|s_1 - s_2\|_H^2 \\ &= -2\langle s_1, s_2 - s_1 \rangle_H - 2\langle s_2, s_1 - s_2 \rangle_H \\ &= -2\langle s_1, s_2 - s_1 \rangle_H - 2\langle s_2, s_1 - s_2 \rangle_H \\ &\quad - \int_{\Omega} \Delta(s_2 - s_1)(x) dx - \int_{\Omega} \Delta(s_1 - s_2)(x) dx \\ &\leq 0 \end{aligned}$$

which shows  $s_1 = s_2$ .

#### Step 5. full sequence is strongly convergent

Finally, we remove the subsequence assumption on  $(v_n)_{n \in \mathbb{N}}$  from Step 1. For a contradiction assume that the original sequence  $(v_n)_{n \in \mathbb{N}}$  does not converge strongly to  $v$ . Then there is an  $\varepsilon > 0$  and a subsequence  $(v_{n_k})$  such that

$$\|v_{n_k} - v\|_H \geq \varepsilon \text{ for all } k \in \mathbb{N}. \quad (44)$$

Since

$$\|v_{n_k} - v\|_H \leq 2C_0,$$

i.e.  $(v_{n_k} - v)_{k \in \mathbb{N}}$  is bounded, it has a weakly convergent subsequence, but then necessarily  $v_{n_k}$  converges weakly to  $v$ , as we have just shown that every subsequence of  $v_n$  converges to the unique minimizer  $v$ . This is a contradiction to (44) and thus the original sequence converges strongly to  $v$ .  $\square$

Received May 2020; revised October 2020.

*E-mail address:* [P.A.Giesl@sussex.ac.uk](mailto:P.A.Giesl@sussex.ac.uk)

*E-mail address:* [langhornez@yahoo.co.uk](mailto:langhornez@yahoo.co.uk)

*E-mail address:* [carlos@hi.is](mailto:carlos@hi.is)

*E-mail address:* [shafstein@hi.is](mailto:shafstein@hi.is)

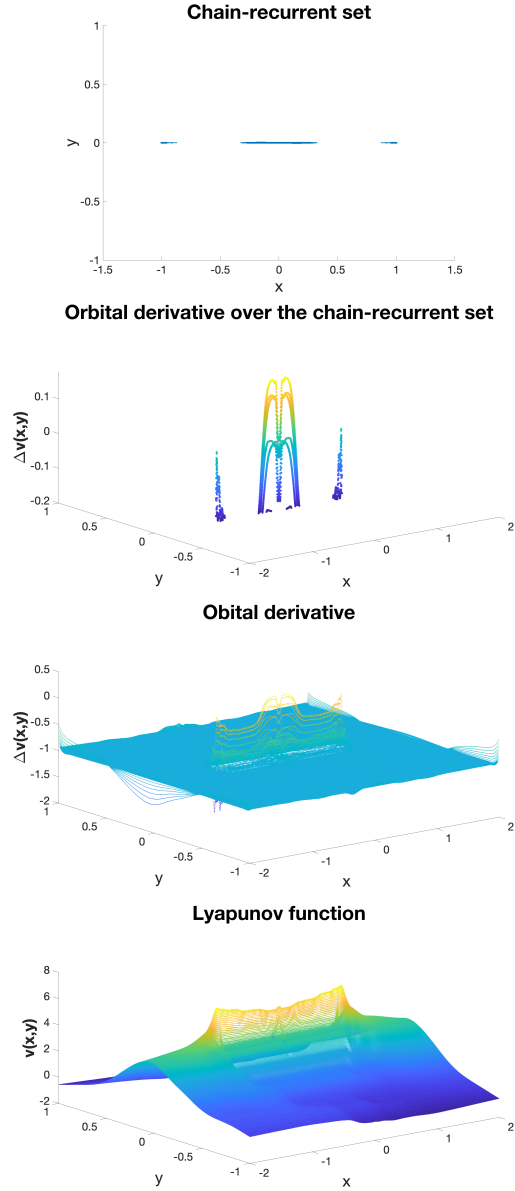


FIGURE 4. Example (25) with solving  $\Delta v(x, y) = -1$ . Chain-recurrent set (top) approximated by the set  $\{(x, y) \mid \Delta v(x, y) \geq \gamma\}$ , see Table 2, and the orbital derivative (second)  $\Delta v(x, y)$  of the constructed complete Lyapunov function  $v$  over the chain-recurrent set. The third figure shows the orbital derivative in a larger set. The approximated chain-recurrent set includes the equilibria at the origin and  $(\pm 1, 0)$ , but is much larger, in particular around the origin. Bottom: Constructed complete Lyapunov function  $v(x, y)$ , which has a saddle point at the origin and a local maximum at the unstable equilibria  $(\pm 1, 0)$ .

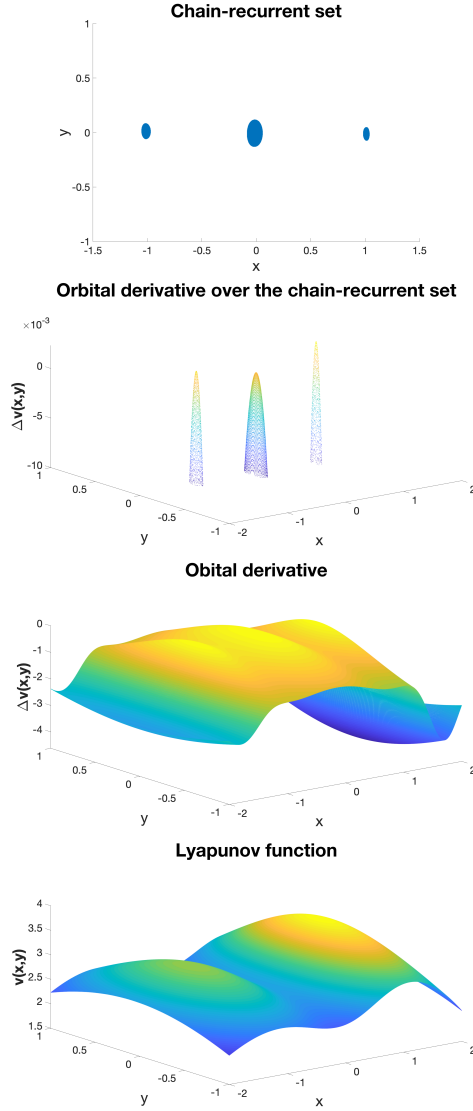


FIGURE 5. Example (25) with equality and inequality constraints. Chain-recurrent set (top) approximated by the set  $\{(x, y) \mid \Delta v(x, y) \geq \gamma\}$ , see Table 2, and the orbital derivative (second)  $\Delta v(x, y)$  of the constructed complete Lyapunov function  $v$  over the chain-recurrent set. The third figure shows the orbital derivative in a larger set.  $\Delta v$  is approximately zero on the chain-recurrent set, consisting of three equilibria at the origin and  $(\pm 1, 0)$ , and negative everywhere else. The approximation of the chain-recurrent set (the equilibria) is much better than when solving the equation  $\Delta v(x, y) = -1$ . Bottom: Constructed complete Lyapunov function  $v(x, y)$ , which has a saddle point at the origin and local maxima at the unstable equilibria  $(\pm 1, 0)$ . Note that they have different levels, which is due to the extra point with equality constraint at  $(0.5, 0)$ , resulting in an unsymmetric approximation.

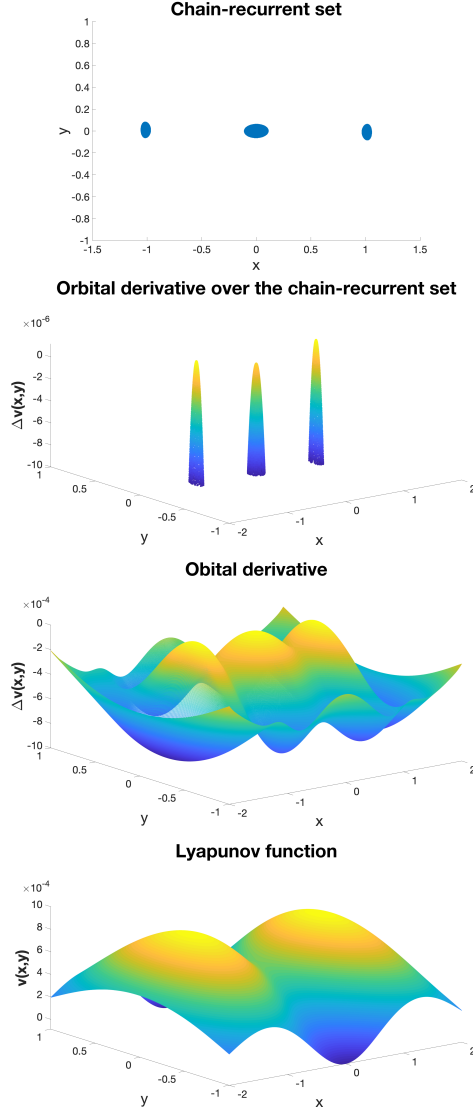


FIGURE 6. Example (25) with inequality constraints. Chain-recurrent set (top) approximated by the set  $\{(x, y) \mid \Delta v(x, y) \geq \gamma\}$ , see Table 2, and the orbital derivative (second)  $\Delta v(x, y)$  of the constructed complete Lyapunov function  $v$  over the chain-recurrent set. The third figure shows the orbital derivative in a larger set.  $\Delta v$  is approximately zero on the chain-recurrent set, consisting of three equilibria at the origin and  $(\pm 1, 0)$ , and negative everywhere else. The approximation of the chain-recurrent set (the equilibria) is much better than when solving the equation  $\Delta v(x, y) = -1$ . Bottom: Constructed complete Lyapunov function  $v(x, y)$ , which has a saddle point at the origin and local maxima at the unstable equilibria  $(\pm 1, 0)$ .

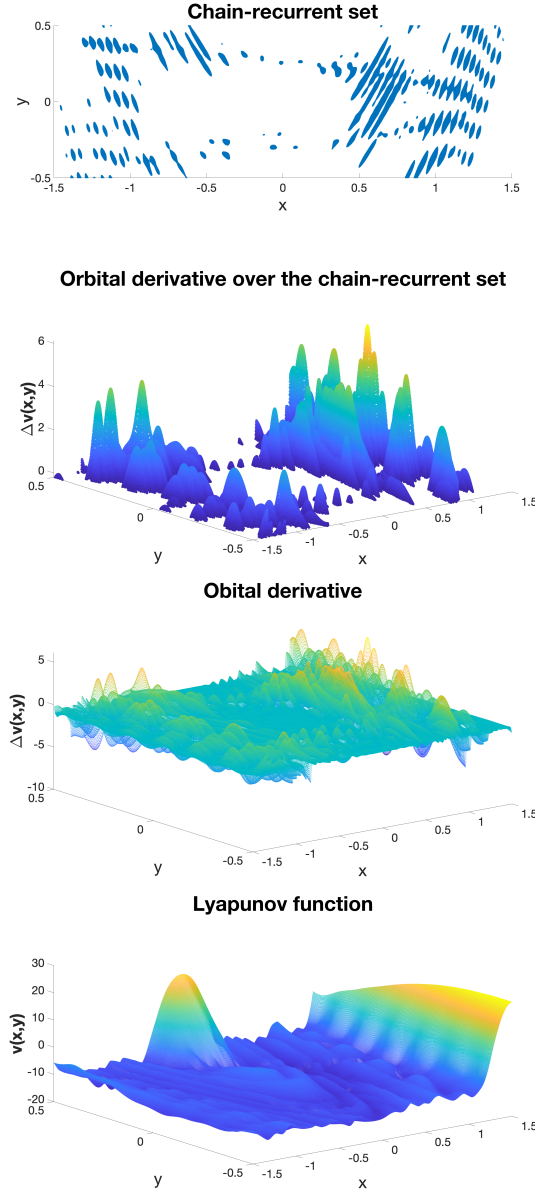


FIGURE 7. Example (26) with solving  $\Delta v(x, y) = -1$ . Chain-recurrent set (top) approximated by the set  $\{(x, y) \mid \Delta v(x, y) \geq \gamma\}$ , see Table 2, and the orbital derivative (second)  $\Delta v(x, y)$  of the constructed complete Lyapunov function  $v$  over the chain-recurrent set. The third figure shows the orbital derivative in a larger set. Bottom: Constructed complete Lyapunov function  $v(x, y)$ . The approximated chain-recurrent set does not resemble the Hénon attractor very well, neither using the orbital derivative nor as the local minimum of the constructed function.

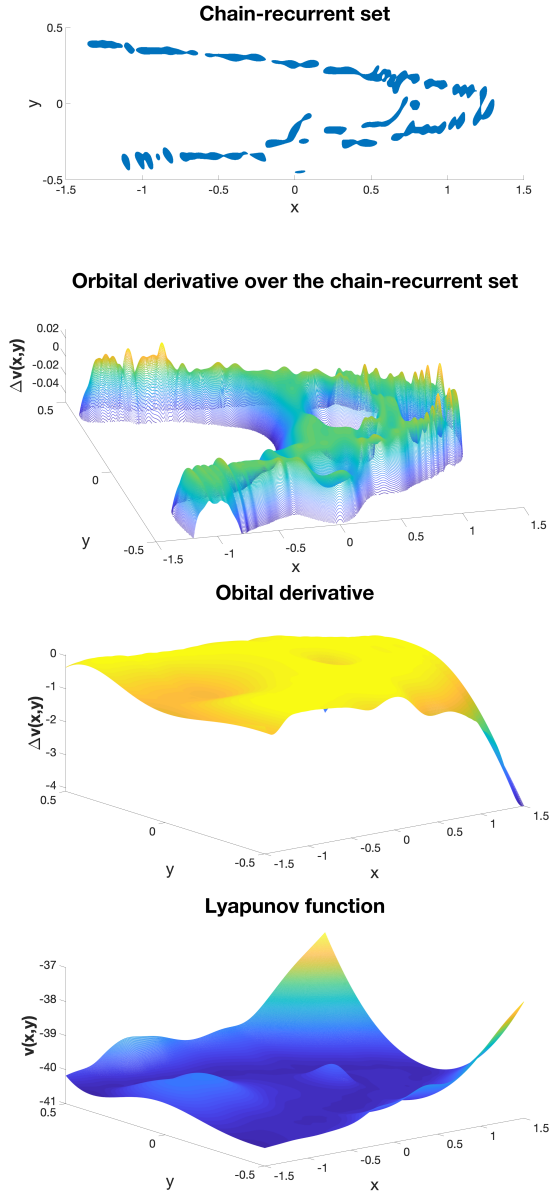


FIGURE 8. Example (26) with equality and inequality constraints. Chain-recurrent set (top) approximated by the set  $\{(x, y) \mid \Delta v(x, y) \geq \gamma\}$ , see Table 2, and the orbital derivative (second)  $\Delta v(x, y)$  of the constructed complete Lyapunov function  $v$  over the chain-recurrent set. The third figure shows the orbital derivative in a larger set. The characteristic shape of the Hénon attractor is clearly visible. Bottom: Constructed complete Lyapunov function  $v(x, y)$  with a local minimum at the Hénon attractor. The point with equality constraint was  $(0.5, 0)$ .

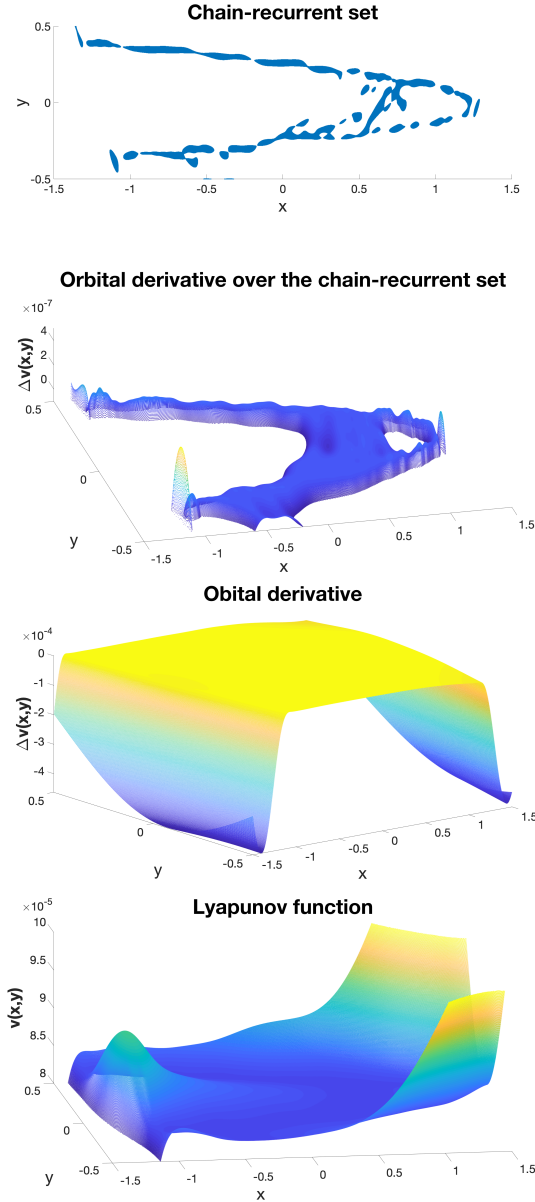


FIGURE 9. Example (26) with inequality constraints. Chain-recurrent set (top) approximated by the set  $\{(x, y) \mid \Delta v(x, y) \geq \gamma\}$ , see Table 2, and the orbital derivative (second)  $\Delta v(x, y)$  of the constructed complete Lyapunov function  $v$  over the chain-recurrent set. The third figure shows the orbital derivative in a larger set. The characteristic shape of the Hénon attractor is clearly visible. Bottom: Constructed complete Lyapunov function  $v(x, y)$  with a local minimum at the Hénon attractor.

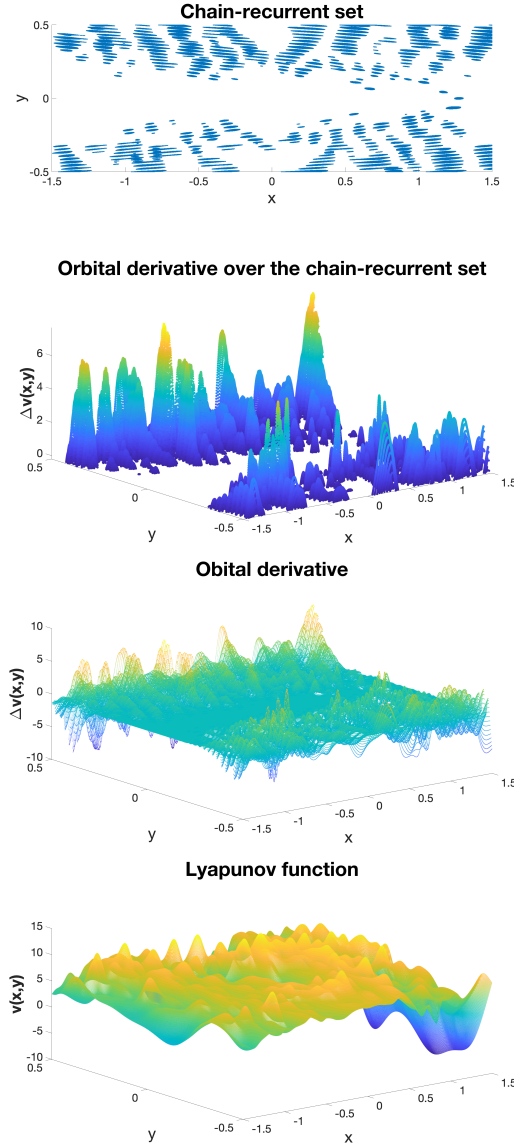


FIGURE 10. Example (27) with solving  $\Delta v(x,y) = -1$ . Chain-recurrent set (top) approximated by the set  $\{(x,y) \mid \Delta v(x,y) \geq \gamma\}$ , see Table 2, and the orbital derivative (second)  $\Delta v(x,y)$  of the constructed complete Lyapunov function  $v$  over the chain-recurrent set. The third figure shows the orbital derivative in a larger set. Bottom: Constructed complete Lyapunov function  $v(x,y)$ . The approximated chain-recurrent set shows the Hénon repeller better than the Hénon attractor in the previous example, but still not very clearly. It is not clearly visible as local maximum of the constructed function either.

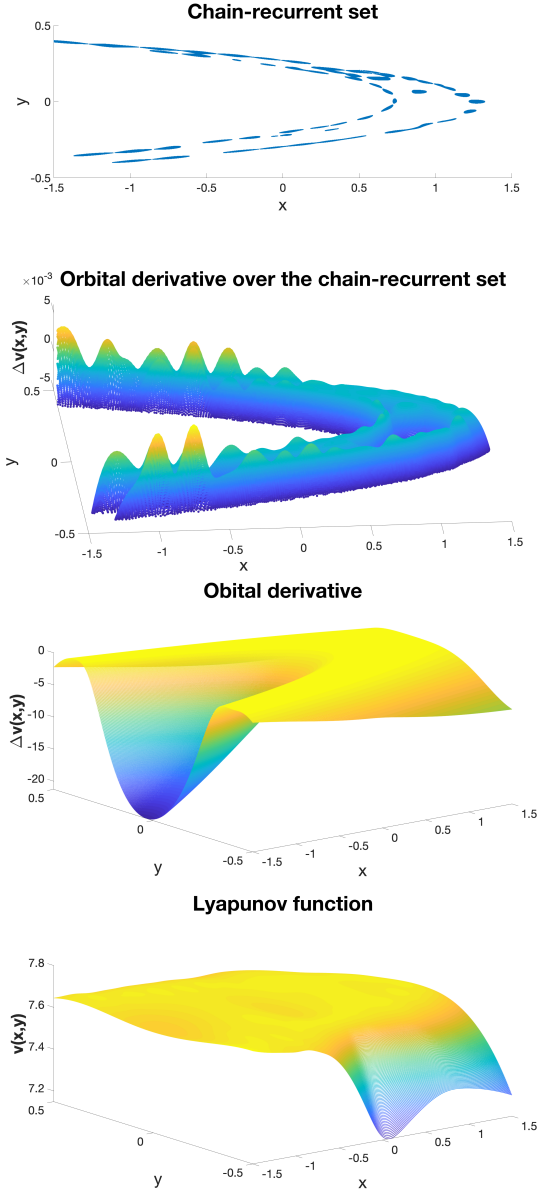


FIGURE 11. Example (27) with equality and inequality constraints. Chain-recurrent set (top) approximated by the set  $\{(x, y) \mid \Delta v(x, y) \geq \gamma\}$ , see Table 2, and the orbital derivative (second)  $\Delta v(x, y)$  of the constructed complete Lyapunov function  $v$  over the chain-recurrent set. The third figure shows the orbital derivative in a larger set. Bottom: Constructed complete Lyapunov function  $v(x, y)$ , showing the Hénon repeller as a local maximum. The repeller is clearly visible in all figures. The point with equality constraint was  $(0.5, 0)$ .

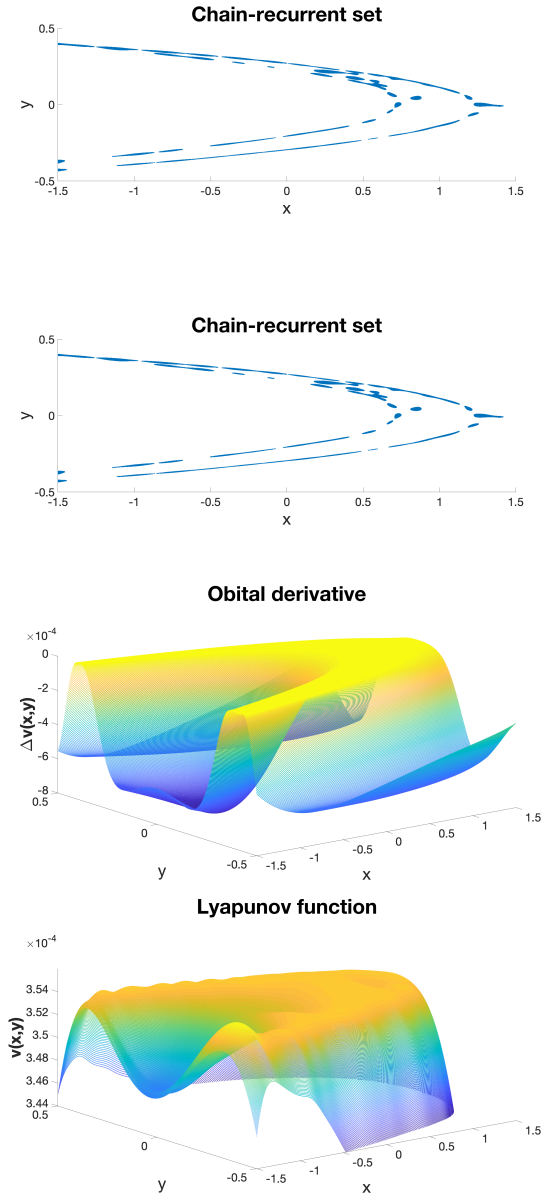


FIGURE 12. Example (27) with inequality constraints. Chain-recurrent set (top) approximated by the set  $\{(x, y) \mid \Delta v(x, y) \geq \gamma\}$ , see Table 2, and the orbital derivative (second)  $\Delta v(x, y)$  of the constructed complete Lyapunov function  $v$  over the chain-recurrent set. The third figure shows the orbital derivative in a larger set. Bottom: Constructed complete Lyapunov function  $v(x, y)$ , showing the Hénon repeller as a local maximum. The repeller is clearly visible in all figures.

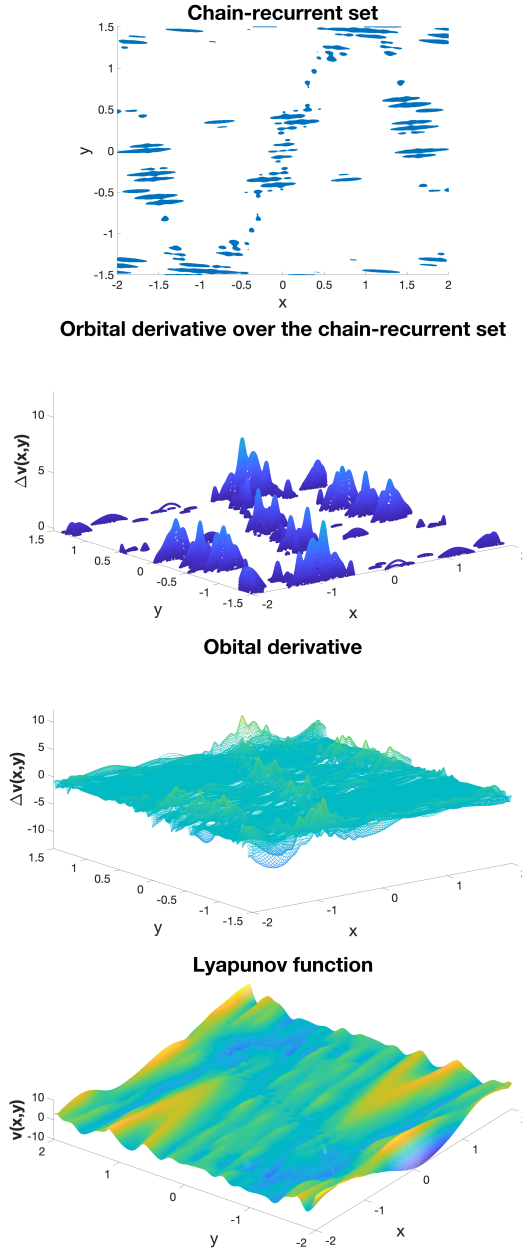


FIGURE 13. Example (28) with solving  $\Delta v(x, y) = -1$ . Chain-recurrent set (top) approximated by the set  $\{(x, y) \mid \Delta v(x, y) \geq \gamma\}$ , see Table 2, and the orbital derivative (second)  $\Delta v(x, y)$  of the constructed complete Lyapunov function  $v$  over the chain-recurrent set. The third figure shows the orbital derivative in a larger set. Bottom: Constructed complete Lyapunov function  $v(x, y)$ . The approximated chain-recurrent set shows the attractor relatively well in the orbital derivative, but not very clearly as local minimum of the constructed function.

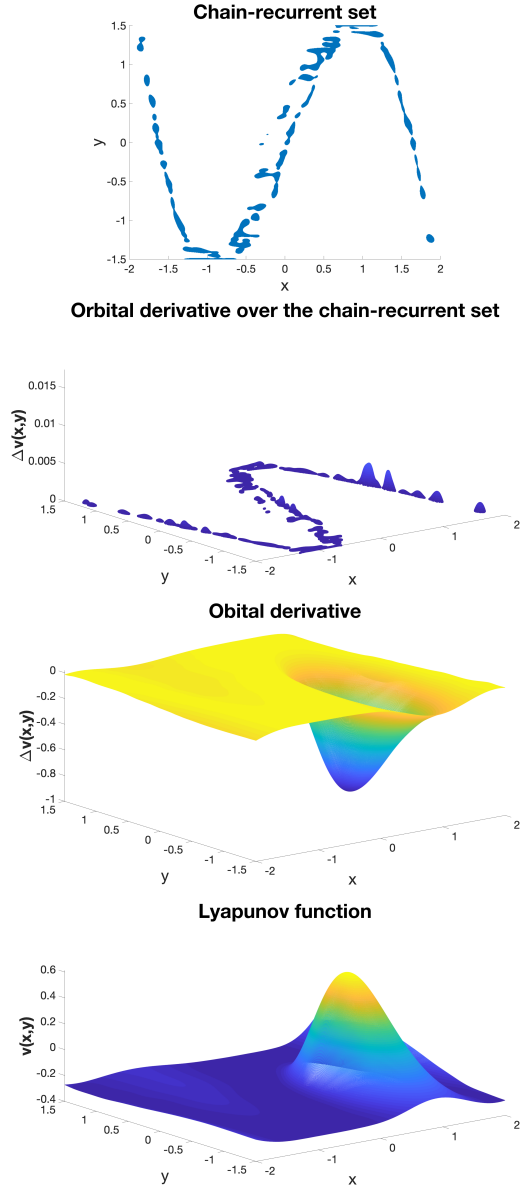


FIGURE 14. Example (28) with equality and inequality constraints. Chain-recurrent set (top) approximated by the set  $\{(x, y) \mid \Delta v(x, y) \geq \gamma\}$ , see Table 2, and the orbital derivative (second)  $\Delta v(x, y)$  of the constructed complete Lyapunov function  $v$  over the chain-recurrent set. The third figure shows the orbital derivative in a larger set. Bottom: Constructed complete Lyapunov function  $v(x, y)$ , showing the attractor as a local minimum. The attractor is clearer than in the previous method, both using the orbital derivative and as local minimum of the constructed function. The point with equality constraint was  $(0.5, 0)$ , where the orbital derivative is fixed at  $-1$ .

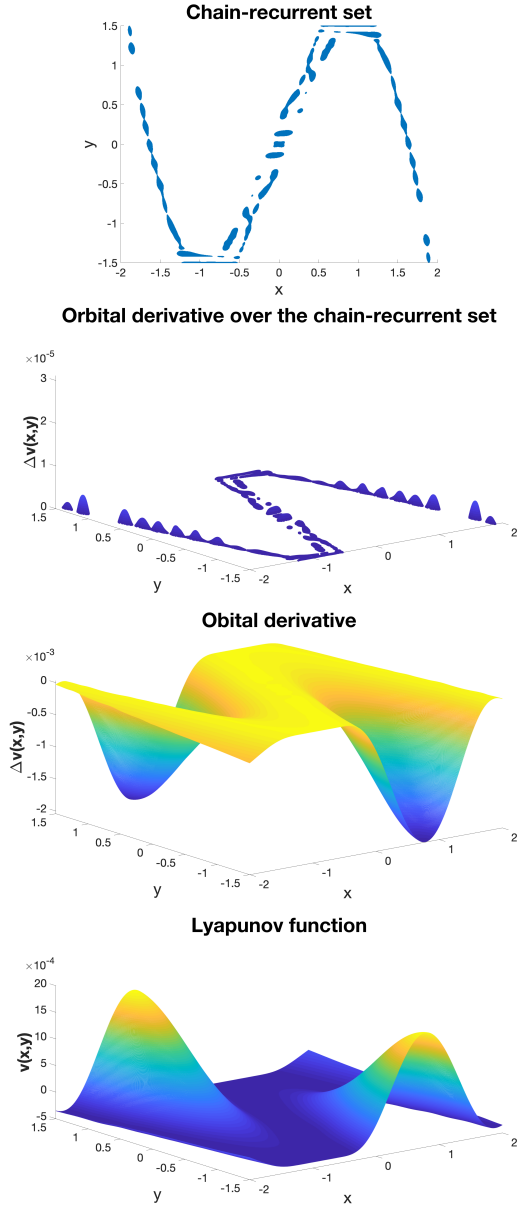


FIGURE 15. Example (28) with inequality constraints. Chain-recurrent set (top) approximated by the set  $\{(x, y) \mid \Delta v(x, y) \geq \gamma\}$ , see Table 2, and the orbital derivative (second)  $\Delta v(x, y)$  of the constructed complete Lyapunov function  $v$  over the chain-recurrent set. The third figure shows the orbital derivative in a larger set. Bottom: Constructed complete Lyapunov function  $v(x, y)$ , showing the attractor as a local minimum. The attractor is clearer than in the first method, both using the orbital derivative and as local minimum of the constructed function.

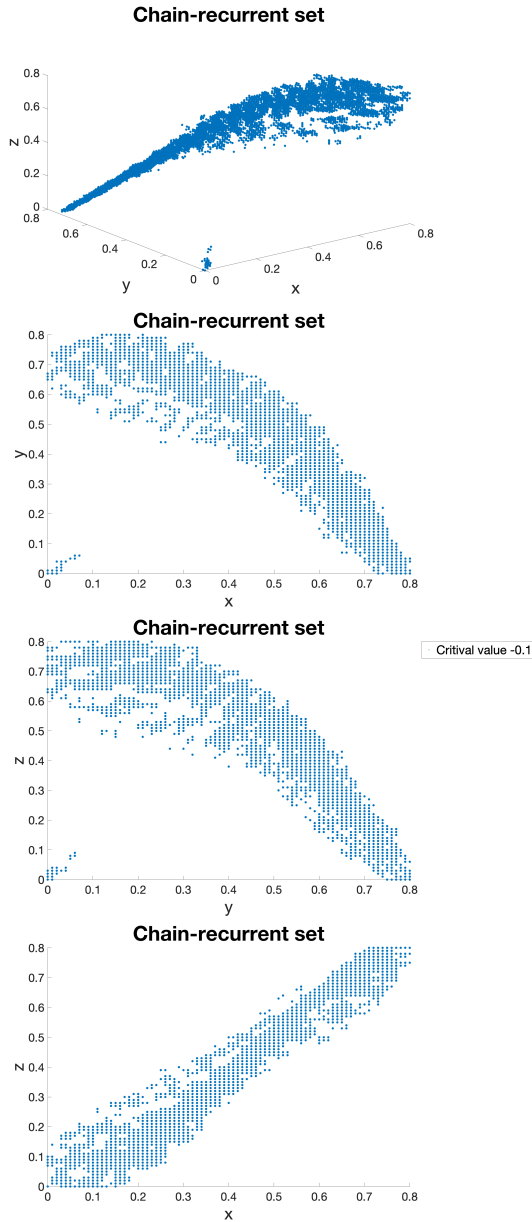


FIGURE 16. Example (29) with solving  $\Delta v(x, y, z) = -1$ .  
 Top: Chain-recurrent set approximated by the set  $\{(x, y, z) \mid \Delta v(x, y, z) \geq \gamma\}$ , see Table 2. The other figures show projections of this set: projections to the  $xy$ - (second),  $yz$ - (third) and  $xz$ -plane (bottom).

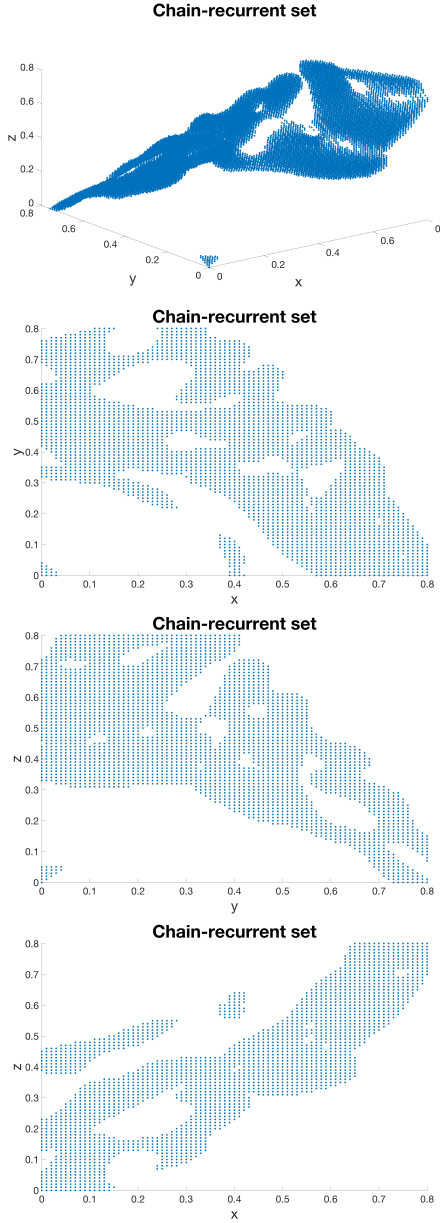


FIGURE 17. Example (29) with equality-inequality constrains. Top: Chain-recurrent set approximated by the set  $\{(x, y, z) \mid \Delta v(x, y, z) \geq \gamma\}$ , see Table 2. The other figures show projections of this set: projections to the  $xy$ - (second),  $yz$ - (third) and  $xz$ -plane (bottom). The figures are not as good as with the previous method. The point with equality constraint is  $(0.4, 0.4, 0)$ .

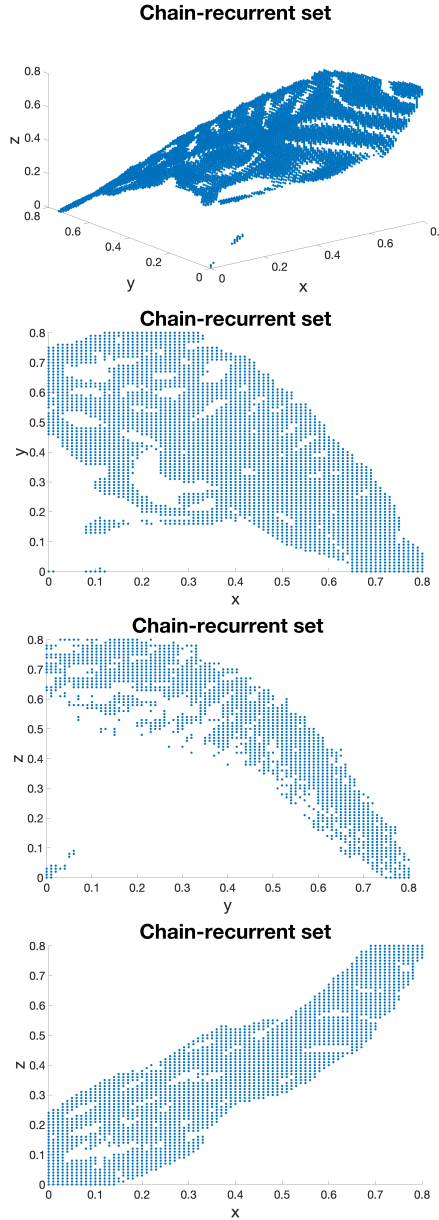


FIGURE 18. Example (29) with inequality constrains. Top: Chain-recurrent set approximated by the set  $\{(x, y, z) \mid \Delta v(x, y, z) \geq \gamma\}$ , see Table 2. The other figures show projections of this set: projections to the  $xy$ - (second),  $yz$ - (third) and  $xz$ -plane (bottom).